

NPS-57NT72031A

//
NAVAL POSTGRADUATE SCHOOL
Monterey, California



Nonmetallized Composite
Propellant Combustion

by

D. W. Netzer, J. R. Kennedy,
G. M. Biery II, W. E. Brown

1 March 1972

Approved for public release; distribution unlimited.

FEDDOCS
D 208.14/2:NPS-57NT72031A

12/8

NAVAL POSTGRADUATE SCHOOL
Monterey, California

Rear Admiral A. S. Goodfellow, Jr.
Superintendent

M. U. Clauser
Academic Dean

ABSTRACT:

An experimental investigation of nonmetallized composite propellant combustion in standard and high acceleration environments was made. Pressed ammonium perchlorate (AP) pellets of varying purity, AP/binder sandwich burners, and propellant strands were employed. AP/binder sandwich burners were studied in an optically equipped centrifuge and color schlieren were taken in a conventional combustion bomb. As-cast and dewetted propellants were used to study the effect of preferential interfacial reactions on burning rate acceleration sensitivity. Results are discussed for the effects of acceleration, pressure, AP purity, and propellant composition on the burning rate.

ACKNOWLEDGEMENTS

This work was sponsored by Naval Ordnance Systems Command, ORD TASK 331 007/551 1/UF 19-332-303. Appreciation is also expressed to Dr. David Flanigan of the Thiokol Chemical Corporation, Huntsville, to Dr. G. B. Northam of the NASA Langley Research Center and to Thomas L. Boggs of the Naval Weapons Center, China Lake for supplying the needed propellants and propellant sandwich ingredients. Mr. Boggs also made possible the needed use of the Naval Weapons Center's scanning electron microscope. Appreciation is also expressed to Mr. Edward Michelson for his assistance in conducting the experiments and to LCDR James Wood for his assistance with the propellant dewetting experiments.

ABSTRACT

An experimental investigation of nonmetallized composite propellant combustion in standard and high acceleration environments was made. Pressed ammonium perchlorate (AP) pellets of varying purity, AP/binder sandwich burners, and propellant strands were employed. AP/binder sandwich burners were studied in an optically equipped centrifuge and color schlieren were taken in a conventional combustion bomb. As-cast and dewetted propellants were used to study the effect of preferential interfacial reactions on burning rate acceleration sensitivity. Results are discussed for the effects of acceleration, pressure, AP purity, and propellant composition on the burning rate.

TABLE OF CONTENTS

	page
I. INTRODUCTION	1
II. METHOD OF INVESTIGATION	5
III. EXPERIMENTAL APPARATUS AND PROCEDURES	8
A. Propellant Specifications	8
B. High Acceleration Centrifuge and Strand Methods	8
C. Optical Centrifuge and Sandwich Techniques	9
D. Combustion Bomb	11
E. AP Pellet and Wafer Fabrication	12
F. AP Pellet Preparation and Testing	14
G. AP/PBAA Sandwich Fabrication	15
H. Propellant Dewetting	16
IV. RESULTS AND DISCUSSION	19
A. Ammonium Perchlorate Deflagration	19
B. Cinematographic Study of AP/PBAA Sandwich Burners	22
C. Schlieren Study of Sandwich Combustion	26
D. A Study of Preferential Interfacial Reactions and Surface Accumulation Effects	31
V. CONCLUSIONS	39
VI. REFERENCES	42
TABLES	45
FIGURES	60
DISTRIBUTION LIST	104

LIST OF TABLES

TABLE		Page
I	Summary of Observed Behavior In Acceleration Environments for Nonmetallized Composite Propellants	45
II	Proposed Models and/or Mechanisms for Acceleration Sensitivity of Nonmetallized Composite Propellants	46
III	AP Specifications	47
IV	Propellant Specifications	48
V	Pure AP Pellet Results	49
VI	Propellant Grade AP (with TCP) Pellet Results	52
VII	Propellant Grade AP Pellet Results	53
VIII	Summary of Data from AP(UHP)/PBAA Sandwich Tests	54
IX	Summary of Data from AP(TCP)/PBAA Sandwich Tests	55
X	Summary of Data from AP(UHP)/PBAA Single Bonded Face Sandwich Test	56
XI	Summary of Incremental Burning Rates for AP(UHP)/PBAA Sandwich Tests	57
XII	Effect of Strand Cross-section on Augmentation of Propellant B-1.	58
XIII	Summary of Data for As-Cast and Dewetted Propellants	59

LIST OF FIGURES

Figure		Page
1	Method of Investigation	60
2	Experimental Apparatus	61
3	Photomicrographs of AP crystals	62
4	Schematic of Sandwich Burner	63
5	Combustion Bomb End Cap with Sandwich Burner Mounted	64
6	View of Assembled Base Section of Combustion Bomb	65
7	View of Assembled Combustion Bomb Along Optical Axis	65
8	Schematic of Combustion Bomb	66
9	Angular Relationship of Bomb Windows	67
10	Electrical Schematic of Combustion Bomb Control Panel	68
11	Scanning Electron Microscope Photomicrographs of High Purity AP Pellet Surface	69
12	Scanning Electron Microscope Photomicrographs of Propellant Grade AP (with TCP) Pellet Surface	72
13	Scanning Electron Microscope Photomicrographs of High Purity AP Pellet Internal Structure	75
14	Scanning Electron Microscope Photomicrographs of Propellant Grade AP (with TCP) Pellet Internal Structure	78
15	Void Formation Upon Dewetting	81
16	Dilatation vs. Stress and Strain for Propellant B-1	82
17	Dilatation vs. Stress and Strain for Propellant B-2	83

18	Dilatation vs. Stress and Strain for Propellant N-3	84
19	Stress vs. Strain for Propellant B-1	85
20	Stress vs. Strain for Propellant B-2	86
21	Stress vs. Strain for Propellant N-3	87
22	AP Burning Rate vs. Pressure	88
23	Photograph of Self-Extinguished AP pellets	89
24	Burn Profiles of AP(UHP)/PBAA Sandwich Tests (Typical frames from high speed motion pictures)	90
25	Burn Profiles of AP(TCP)/PBAA Sandwich Tests (Typical frames from high speed motion pictures)	92
26	Color Photograph of PBAA/AP Sandwich Burning at 800 psi	94
27	Color Schlieren of PBAA/AP Sandwich Burning at 800 psi	94
28	Color Photograph of PBAA/AP Sandwich Burning at 500 psi	95
29	Color Schlieren of PBAA/AP Sandwich Burning at 500 psi	95
30	Color Photograph of PBAA/AP Sandwich Burning at 200 psi	96
31	Color Schlieren of PBAA/AP Sandwich Burning at 200 psi	96
32	Color Photograph of PBAA/AP Sandwich Burning at 100 psi	97
33	Color Schlieren of PBAA/AP Sandwich Burning at 100 psi	97
34	Color Schlieren of PBAA/AP Sandwich Burning at 100 psi, Horizontal Color Matrix	98
35	Color Photograph of PBAA/AP Sandwich Burning at 500 psi, Side View	98
36	Burning Rate vs Pressure for Propellant B-1	99

37	Augmentation vs. Burn Time for Propellant B-1	100
38	Augmentation vs. Acceleration for Propellant B-1	101
39	Augmentation vs. Acceleration for Propellant B-2	102
40	Augmentation vs. Acceleration for Propellant N-3	103

I. INTRODUCTION

The burning rate acceleration sensitivity of solid propellants has been studied both experimentally and analytically during the past ten years. Most attention has been directed toward metallized composite propellants. Nonmetallized composite propellants have received far less attention and very little work has been reported for double base propellants.

The primary mechanism responsible for the acceleration sensitivity of many metallized composite propellants (operating at normal pressures and with nominal burning rates) has been shown to be the acceleration induced retention of metallic agglomerates on the burning surface (3, 10, 15, 20, 21). This phenomenon has been modeled with limited success (10, 23). However, there are some notable limitations of the analytical model(s). The two primary limitations of the model are its inability to handle the experimentally observed transient burning rate phenomena (3, 10, 15, 20, 21) and the acceleration sensitivity that results from other than metallic agglomerate effects (1, 3, 15, 16). The latter phenomena are also responsible for the acceleration sensitivity of nonmetallized propellants and are not well understood.

Table I presents a summary of the major experimental findings related to the acceleration sensitivity of nonmetallized composite propellants. A review of Table I indicates that, in general, in an acceleration environment nonmetallized composite propellants behave in a similar

fashion to metallized composite propellants. However, the mechanism(s) responsible for the burning rate acceleration sensitivity is, in most cases, significantly different. The dominance of the base (zero g) burning rate on the acceleration sensitivity is identical for both metallized and nonmetallized propellants.

The apparently conflicting results shown in Table I for the effect of metal content, the possible effect of binder composition and the recent results of Northam (16) and Cowles and Netzer (15) indicate that little is known about the causes for the acceleration sensitivity of nonmetallized composite propellants. Intuitively, there are several possible mechanisms that could be responsible for the burning rate acceleration sensitivity, and the mechanism may be different for different propellant ingredients and/or test environments. Possible mechanisms include:

(a) preferential interfacial reactions that may free the ammonium perchlorate (AP) from the binder (3), (b) AP deflagration/surface melt, (c) binder melt and its interaction with the AP and/or AP surface melt, (d) gas phase phenomena at high accelerations and (e) impurities in the AP or binder which may act directly or accumulate on the burning surface (TCP, carbon, etc).

Table II lists the models and/or mechanisms that have been proposed and comments on their validity. The various models have been discussed elsewhere (9, 15). In general, existing experimental data are not adequate for determining the dominate mechanism(s) responsible for the burning rate acceleration sensitivity of nonmetallized composite propellants.

Whichever phenomena are significant in producing the burning rate acceleration sensitivity of these propellants, it should be expected that results from Og studies will be of considerable importance in any attempted modeling of the acceleration effects. Many models have been proposed for the combustion of composite propellants and have been summarized by numerous authors (17). The various models are based upon different proposed physical phenomena and no general agreement has been reached concerning which of the models most nearly represent the actual burning mechanism(s).

One experimental technique currently being used to study composite propellant combustion consists of concurrent use of high speed motion pictures and rapid quenching of propellant sandwiches (26, 28, 33, etc). These two-dimensional propellants allow the binder/AP interactions to be studied over a wide variety of test conditions and propellant ingredients. However, the direct application of sandwich propellant results to actual propellant behavior remains in question. Boggs and Zurn (28) have discussed the advantages and disadvantages of using sandwich burners to study composite propellant combustion.

The existence and importance of binder and AP surface melts during combustion have been reported (18, 19, 24, 28). AP surface melts may explain the various reported regimes of AP deflagration as pressure is increased (24, 30, 32). These studies have also noted the lack of evidence for preferential subsurface interfacial reactions between the binder and ammonium perchlorate. For PBAA/AP sandwich burners (among others), PBAA melt has been observed to flow over the adjacent AP for

distances up to 150μ (17). Studies of actual propellant combustion (18) have also shown that at low pressures, AP may protrude above the burning surface and at high pressure it may be recessed below the surface. These findings suggest that binder/AP surface melts and their interactions may be of added significance in acceleration environments.

The purposes of this investigation were to determine the dominate acceleration sensitive mechanism(s) in nonmetallized composite propellant combustion and to obtain a better description of solid propellant combustion in nominal (0g) acceleration environments. Both are necessary for realistic modeling.

II. METHOD OF INVESTIGATION

The approach employed in this investigation was to attempt to separate the various possible acceleration sensitive mechanisms in the combustion of nonmetallized composite propellants. The overall investigation is outlined in Figure 1. The experimental apparatus employed and the type of experiments conducted are briefly outlined in Figure 2. Details are presented in Section III.

In an attempt to determine whether preferential interfacial reactions exist and result in burning rate acceleration sensitivity, several propellants were tested in strand configurations at 500 psia with accelerations to $\pm 1000g$ (normal and into and normal and out from the burning surface). Each propellant was burned in both the as-cast condition and in a prestressed (dewetted) condition.

The as-cast and dewetted conditions provided two propellants which were identical in all respects except that the interfacial conditions of many of the larger AP crystals were radically different. If interfacial reactions and/or "free-AP" (3) is one of the mechanisms responsible for burning rate acceleration sensitivity, then the two propellants would be expected to behave differently in an acceleration environment and also possibly at zero g.

These same propellants were also burned at zero-g with pressures from 250 to 1000 psia in order that relative propellant characteristics (pressure exponent, etc.) could be compared.

To determine the possible existence of surface accumulation/transient phenomena, the as-cast propellants were also burned in acceleration

environments with varying strand length and cross-sectional area.

Another phase of the investigation was concerned with the possible acceleration sensitivity of AP deflagration with its associated surface melt. To study this effect, pressed AP pellets were burned from pressures of 400 to 800 psia with accelerations to $\pm 1000g$. Ultra-high purity AP, propellant grade AP, and propellant grade AP with TCP conditioner were utilized to determine the effect of impurities. The purposes of this study were (a) to determine if AP deflagration is acceleration sensitive and if so, to what extent would it influence the burning rate acceleration sensitivity of composite propellants and (b) to provide additional information about the existence and behavior of AP surface melt in the AP deflagration process.

The third phase of the investigation was concerned with the interactions of the AP/AP melt with the binder/binder melt. Acceleration induced mixing of these melts may alter both the surface phenomena and the gas phase reaction zone. These effects in turn may alter the burning rate. This study was conducted using AP/PBAA sandwich burners and consisted of two separate investigations. One investigation was concerned with the behavior of the sandwich burners in an acceleration environment. AP/PBAA sandwiches were burned at $0g$ and $+100g$ with pressures from 200 to 800 psi. Ultra-high purity AP and propellant grade AP with TCP conditioner were used. High speed color motion pictures were taken in a specially equipped centrifuge. These tests allowed burning rates to be determined and physical phenomena (melt interactions, etc) to be visually observed.

A second phase of the sandwich combustion study was concerned with the behavior of the gas phase combustion process. AP deflagration is not visible at pressures below approximately 1500 psi and therefore the gas phase combustion process cannot be adequately studied below this pressure using only standard high speed color photography.

In order to provide a better description of sandwich combustion, high speed color schlieren were taken of AP/PAA sandwiches burning in standard gravity conditions with pressures from 100 to 800 psi. These tests allowed the AP deflagration to be observed as well as the interaction of the binder and AP decomposition products.

III. EXPERIMENTAL APPARATUS AND PROCEDURES

A. Propellant Specifications

Specifications for the ammonium perchlorate utilized in this investigation are shown in Table III and photomicrographs are presented in Figure 3.

Propellant specifications are shown in Table IV.

The binder used in the sandwich burners consisted of 84% PBAA and 16% EPON 828 by weight. It was cured for 96 hours at 72C with the first three hours in a vacuum in excess of 28 in Hg.

B. High Acceleration Centrifuge and Strand Methods

Details of the high acceleration centrifuge can be found in References 1, 2, 3, and 8 and only a brief description will be presented. The combustion bomb was mounted on the centrifuge at a three-foot radius, which provided an approximately constant acceleration during the burning process.

All four sides and the base of propellant strands were rigidly inhibited with Selectron 5119 resin and "Garox" curing agent.

The strand was ignited by a thin layer of black powder-glue mixture placed across the propellant surface. The black powder, in turn, was ignited by a nichrome resistance wire adjacent to the propellant surface. Although the ignition current was adjusted so that the wire would not burn out, if burn-out did occur the location of the wire prevented it from falling onto the burning propellant.

The propellant was taped to a strand holder and sealed in the combustion bomb. The initial static pressure was set and the centrifuge was brought to the desired speed. The strand was ignited and a bomb pressure-time trace was recorded with a Visicorder model 1508.

The pressure-time trace typically exhibited a pressure peak and fall-off followed by a steady pressure rise. Burn-out was taken to be the sharp pressure drop after the steady burning process. Average burning rate was determined by dividing the known strand length by burn time measured from the pressure-time trace. The mean pressure of the pressure-time trace was determined in order that the actual mean combustion bomb pressure during the burn process would be known.

C. Optical Centrifuge and Sandwich Techniques

The optically equipped centrifuge has been previously discussed in Reference 8 and will be discussed only briefly. This centrifuge is capable of producing approximately 110 g with the current apparatus mounted on the table. The combustion bomb is nitrogen purged and can be operated to pressures of 800 psi.

Three plexiglass windows are installed in the combustion bomb. Two windows, located diametrically opposite, are separately utilized for cinematographic observation of the propellant sandwich. A General Electric Marc 300/16 projection lamp, and a solenoid operated lamp shutter are mounted above the third window to illuminate the propellant sandwich during filming. The shutter was opened just prior to ignition to prevent inadvertent propellant ignition or excessive heating by the lamp radiation.

Two mirrors and a Pentax Auto-Takumar 3.5, 135 mm lens, were used to project the propellant strand image to a Hycam, model K1001, 16 mm high speed motion picture camera mounted in a stationary position above the rotating table. Kodak Ektachrome EF 7241 Daylight film was used for all color cinematography. The Hycam camera was used with an extension tube adapted to a 50 mm lens which provided approximately a 1.4 magnification factor on the film plane. All runs were made at a framing rate of 1500 pictures per second.

AP/PBAA sandwich burners were glued to an aluminum pedestal as shown in Figure 4.

A pencil mark was made on the edge of one AP crystal of the sandwich. This mark was made 0.15 inch up from the bottom edge of the burner. The pencil mark served the purpose of marking a focal point for the optical axis as well as supplying a reference point on the wafer from which photographic determination of burning rate could be made in the acceleration test. The completed sandwich burner mounted on the combustion bomb end cap is shown in Figure 5. The sandwiches were burned in the horizontal position in the combustion bomb of the photographic centrifuge.

Ignition of the sandwich burners was accomplished using an 0.008 inch diameter nichrome resistance wire over the top of the burner. The wire was so oriented as to lie on the exposed binder at the top of the burner. A black powder / glue / acetone mixture was then applied over the ignition wire to the top of the burner and allowed to dry.

During test the combustion bomb was purged with nitrogen to clear as much smoke as possible from the bomb and to provide an inert atmosphere.

Burning rates were taken from the films by projecting them onto a screen and measuring a length of burn over approximately 0.4 to 0.6 of a second elapsed time. The top 0.075 inch of the sandwich was not included in the burning rate measurements because of varied ignition transients. The average burning rates were calculated from the burn occurring between 0.075 inch from the sandwich top to 0.24 inch from the sandwich bottom. This distance was about 0.080 inch long. The time elapsed between two points on the film was taken by counting the number of 0.001 second timing marks placed on the film edge by a Red Lake Laboratories Millimite TLG-4 timing oscillator.

When burning the sandwiches, sometimes the flame zone on one side of the binder would extend deeper into the burner than on the other side. On some runs this lowest point would shift back and forth from one side of the binder to the other. All burning rate data were taken for the maximum point of advance of the flame zone.

The calculated burning rates are average burning rates for the zone over which the burn was observed.

D. Combustion Bomb

A stainless steel combustion bomb was designed and fabricated for an operating pressure capability of 0 to 1000 psi, and hydrostatically tested to 1500 psi. It was composed of three main sections - base, center (or window), and exhaust. Integral provision was made for mounting AP sandwiches and a nitrogen purge system. Figures 6 and 7 are photographs of the combustion bomb. Figure 8 is a schematic showing principal

dimensions of the assembled bomb. Figure 9 is a schematic showing the angular relationship of the windows in the combustion bomb. Figure 10 is an electrical schematic of the control panel.

A blue-red filter matrix was used in place of a solid knife edge for the schlieren films so that density gradients in both directions would be more visible on the film. In all but one schlieren run the color matrix was placed in the vertical position in order to distinguish density gradients in a direction perpendicular to the flame. All film, both schlieren and normal color photography, were taken at 5000 pictures per second with a 1/2.5 shutter. Kodak Ektachrome 7241 high speed color film was used in the Hycam camera.

A 203 mm, f 7.7 lens was used to focus the sandwich image directly onto the film plane. The light source for the schlieren was a 1000 watt mercury arc lamp. Side lighting was also provided by a 625 watt television flood light. The high speed color films (non-schlieren) were taken using the above 625 watt light together with a modified Spindler and Sauppe SIM-1200, 1200 watt slide projector.

All but one run were made with the binder plane aligned with the optical axis.

E. AP Pellet and Wafer Fabrication

Ammonium perchlorate was pressed into pellets or wafers using compaction molds similar to that used by Varney (17). The one-half inch diameter pellets and the one-inch diameter wafers were fabricated with thicknesses of approximately 0.25 and 0.050 inch respectively.

The initial pellets and wafers were fabricated with a technique similar to that used by Varney (17). The AP was ground with a mortar and pestle and then placed in a compaction mold at 30,000 - 30,500 psi for 24 hours.

Subsequently, AP pellets and wafers were fabricated with a simplified procedure. The as-received AP was placed directly into the compaction mold without grinding and held at 30,000 - 30,500 psi for 20 minutes.

Calculated density of the AP pellets was in excess of 1.94 gm/cm^3 (better than 99 percent of crystalline density) for both the ground/24 hour method and the unground/20 minute method of fabrication. The burning rate of the pellets did not change appreciably when the fabrication technique was changed. Measured burning rates (of .177 in/sec) at 500 psia were obtained which compared favorably with single crystal AP burning rate (17, 30). Based upon these results all subsequent wafer and pellet fabrication utilized the unground AP and a 20 minute compaction at 30,000 - 30,500 psi. AP wafers fabricated with this technique had densities in excess of 1.92 gm/cm^3 (98 percent of crystalline density).

A scanning electron microscope (Naval Weapons Center, China Lake) was used to examine the as molded surface and interior structure of the AP pellets. Figures 11 and 12 present the scanning electron microscope (SEM) photomicrographs for the as molded surfaces of AP pellets made with ultra-high purity AP and propellant grade AP with

TCP conditioner respectively. Figures 13 and 14 present the corresponding SEM photomicrographs of the interior structure of the pellets (taken from cleaved pellets). The photomicrographs indicated that very few voids existed in the pellets when made with a pressure in excess of 30,000 psi. A significant difference in the microstructure of the pellets made with the AP(UHP) and the propellant grade AP with TCP additive is evident. This difference is due in part to the differing AP size and configuration (rounded) and may also be affected by the TCP and/or ash in the propellant grade AP. All pellets and wafers were translucent and white in appearance. The surfaces were visually glossy and very smooth. The pellets and wafers made with the propellant grades of AP had a visual appearance that was more granular and chalky white than those made with ultra-high purity AP.

F. AP Pellet Preparation and Testing

Except for a few control samples, all pellets were rigidly inhibited with Selectron 5119 on all but the normal burning surface. These pellets were normally burned in a horizontal position in the large centrifuge. Two ignition methods were employed; a nichrome resistance wire placed directly across the AP pellet face, and a black powder/glue/acetone mix placed on the AP face which was ignited by an adjacent nichrome resistance wire.

In order to obtain repeatable results it was necessary to lightly scrape the AP surface that was to be ignited. This procedure removed the glossy finish that existed when the AP was removed from the mold.

There was some concern about the possible effect of the rigid inhibitor on the burning rate. Several tests were conducted in which no inhibitor was used on the sides of the pellets. In general, these tests were unreliable due to burning down the sides of the pellets. When the centrifuge pressure time trace indicated a good burn, the burning rate was found to be essentially the same as that of the rigidly inhibited pellets.

G. AP/PBAA Sandwich Fabrication

AP wafers were bonded together in pairs with PBAA binder to form a sandwich. The binder was prepared by thorough mixing of PBAA with EPON 828 in the ratios of 84 percent by weight to 16 percent by weight respectively. One thousandth inch thick brass shim stock was placed between the AP wafers at three equally spaced points along their edges to ensure uniformity of binder thickness.

The sandwiches were then placed in a constant temperature oven at 72°C under a vacuum bell and were cured for a ninety-six hour period. During the first three hours of the cure period the vacuum bell was evacuated in excess of 28 inches of mercury.

This procedure resulted in binder thicknesses which varied from sandwich to sandwich because the top wafer would rise and fall during the initial vacuum cure.

During later portions of this investigation, small (approximately 15 gram) stainless steel weights were placed on the top AP wafer of the sandwich to further ensure binder thickness uniformity, and to reduce the tendency for the two wafers to slide over one another when the curing jar was evacuated.

Single faced sandwiches (PBAA bonded to one AP wafer only) were constructed by placing the PBAA/EPON 828 mixture on a flat of Teflon or RTV and then placing an AP wafer over the top of the binder. These were cured in the same manner as described above, and were then lifted from the Teflon or RTV for cleaving.

The bonded AP/PBAA sandwiches were cleaved into small burners. These burners were then scraped to produce a squared face all the way around. The final dimensions of the sandwich burners used in the centrifuge were approximately 0.40 inches high by 0.27 inches in depth. The sandwiches used the combustion bomb schlieren work were approximately 0.35 inches high and had a depth in the optical path of 0.15 inches.

H. Propellant Dewetting

As a propellant is loaded beyond a certain critical stress, bonds in the region of the interface between the oxidizer particle and the binder are broken and the binder pulls away from the particle. This results in vacuoles or voids forming along the uniaxial tensile axis of the larger oxidizer particles (Fig. 15). Once the stress is removed, the voids collapse leaving the bonds broken at the interface. The particles remain in this dewetted condition for extended periods of time. Thus, a change in the interfacial characteristics between the large oxidizer particles and the binder is obtained by stressing the propellant.

Dewetting characteristics of the propellants were obtained utilizing a dilatometer and an Instron tensile testing machine.

The dilatometer consisted of a test cavity filled with silicon oil. It was instrumented to measure stress, strain and volume change of the propellant sample undergoing testing. Detailed explanation of the dilatometer and operating procedures may be found in Reference 35. Specimens one-half by one-half inch in cross section and four inches in length were tested in the dilatometer. Specimens were loaded at a constant strain rate to determine stress and strain required before the onset of dewetting.

Once the required stress for onset of dewetting had been determined in the above manner, specimens of the same size were loaded on the Instron tester at the same strain rate to a stress level intermediate between onset of dewetting and failure. After loading and unloading, the specimens were immediately reloaded to verify dewetted stress-strain plots as reported in Reference 36.

Twenty-four hours were required to inhibit and burn propellant strands. Therefore, selected samples of each propellant were retested on the Instron after this period of time to insure that they retained dewetted properties.

Figures 16, 17 and 18 show dilatation (ratio of volume change to original volume) for propellants B-1, B-2 and N-3 respectively. Propellant N-1 data are not presented since no dewetting was evident prior to sample fracture.

No vacuole formation will occur prior to onset of dewetting, and since propellants are typically incompressible, dilatation will be essentially zero until dewetting occurs. At the critical stress for dewetting, dilatation versus stress or strain will become nonlinear.

This nonlinearity will continue until no more void formation occurs. From this point dilatation will become linear with increasing stress. Figure 16 indicates that propellant B-1 dewetted at approximately 25 psi. Figure 17 indicates that propellant B-2 dewetted at approximately 45 psi. The N-3 propellant was observed to dewet almost instantaneously due to the large oxidizer particle size (Fig. 18).

Figures 19, 20 and 21 show the stress-strain curves resulting from tensile testing. All propellants exhibited dewetted curve characteristics (36) on immediate reload and retained their dewetted properties after a twenty-four hour period.

IV. RESULTS AND DISCUSSION

A. Ammonium Perchlorate Deflagration

The discussion will be divided into three sections, ultra-high purity AP results, propellant grade AP with TCP results, and propellant grade AP without TCP results. AP pellet fabrication and testing methods are discussed in sections IIIIE and IIIIF.

A.1 Ultra-High Purity AP Pellets

The results obtained from the ultra-high purity AP pellet combustion study are summarized in Table V. Initially tests were made using a technique similar to that used by Varney (17) because other investigators had found that the initial crystal size used in the pellets affected the burning rate (34) (see section IIIIE). It was found that pellet density (above 99 percent of crystalline density) and burning rate were not appreciably affected when unground crystals were used in place of the powdered AP. Evidently, the high pressures employed to make the pellets eliminated the dependence of burning rate on initial crystal size. The SEM photomicrographs discussed in section IIIIE showed that practically no voids existed in the pellets.

In order to insure a uniform burn across the 0.25 in. diameter pellet face, ignition was accomplished by using a black powder/glue mixture placed across the AP together with an adjacent nichrome resistance wire. In addition, this technique prevented the ignition wire from falling onto the AP surface if it broke or burned during the tests made in an acceleration environment. Tests were conducted with the burning surface in a vertical position.

The pellet burning rate as a function of pressure is shown in Figure 22. The burning rates compare favorably with single crystal AP burning rates (32). The low pressure deflagration limit was found to be greater than 325 psia. As the acceleration level directed normal and into the burning surface (+g) was increased the burning rate decreased slightly and unburned AP began to appear in the bottom of the rigid inhibitor cases. At 500 g the pellets could not be ignited. The ignition procedure left the AP surface in a pitted condition (see the left photograph in Figure 23).

To determine whether the above phenomenon was resulting from surface melt effects, two pellets were modified. One pellet surface was scraped (as shown in Table V) to produce a surface sloped toward the center. Another pellet surface was scraped to produce a surface parallel to the initial surface but recessed below the top of the rigid inhibitor. Both of these pellets were then tested at 500 g. The results are shown in Figure 23 and Table V. The AP began to burn and then extinguished, leaving what appeared to be a recrystallized molten layer of AP on the surface.

Tests conducted with the acceleration directed normal to and out from the burning surface yielded burning rates the same as 0g burning rates.

A series of tests were then made in which the ignition source was a nichrome resistance wire placed directly across the center of the pellet face. The results indicate (Table V) that in general, the burning rates were less than when the surface was uniformly ignited. The time of ignition was difficult to determine for these tests because the initial

rise in bomb pressure was very slow. In addition, the "notch" ignition would be expected to give longer burn times. The most interesting result is that the pellets continued to deflagrate at the high accelerations when only the wire was used for ignition.

These results indicate that a surface melt does exist on the AP surface and that the quantity of the melt may depend upon the ignition energy (or flame zone location, etc. in propellant combustion) and surface configuration. The black powder ignition method evidently causes more melt to be initially present. This additional melt persists throughout the entire burn in an acceleration environment. The acceleration forces the melt against the solid surface, slightly decreasing the burning rate at low acceleration levels and extinguishing the deflagration at high acceleration levels.

The burning rate acceleration sensitivity of AP is opposite to that normally observed for nonmetallized composite propellants. Therefore, AP deflagration by itself cannot be used to explain the acceleration sensitivity of these propellants.

A.2 Propellant Grade AP (with TCP) Pellets

Results of the tests with propellant grade AP pellets are summarized in Table VI. The AP used in these pellets had 0.2% tricalcium phosphate added as an anti-caking agent and also contained 0.40% sulfated ash. For all practical purposes these pellets would not deflagrate. In the four instances when ignition was successful, the pellets had very low burning rates ($< .10$ in/sec). Evidently, the TCP or sulfated ash inhibits the AP deflagration.

A.3 Propellant Grade AP Pellets

Results are summarized in Table VII. The crystal size used in these pellets was very nearly the same as that used in the propellant grade AP with TCP. The major difference was that no TCP was incorporated and the ash content is typically less than .06%. These pellets were more difficult to ignite and burned more slowly than the ultra high purity AP pellets. Since no TCP was contained in these pellets, these results indicate that the sulfated ash may be the impurity that inhibits the deflagration of AP.

B. Cinematographic Study of AP/PBAA Sandwich Burners

The experimental results of this phase of the investigation are summarized in Tables VIII, IX, X, and XI.

The remarks in this section represent a composite of the general and detailed information derived from the films of all runs which could be considered successful.

Figures 24 and 25 show selected frames from runs made for varying "g" loadings, combustion bomb pressures, and AP grade. An edited color film is available on loan from the Naval Postgraduate School.

Sandwich burners fabricated from the propellant grade AP with TCP additive burned less readily than the ultra high purity AP sandwiches at all pressures and "g" loadings, other than at 200 psi. This result is in agreement with the AP pellet data discussed above. It is apparent that at 200 psi, which is below the low pressure deflagration limit (P_{dl}) of AP, there is some mechanism (physical and/or chemical) that causes the commercial grade AP with TCP to be consumed more readily than the ultra high purity AP.

At other pressures above P_{dl} for pure AP, the sandwiches made with ultra high purity AP show higher burning rates in all cases than the corresponding tests with sandwiches made with propellant grade AP with TCP conditioner. Photographic observations show that the ultra high purity AP is self-deflagrating at 500 and 800 psi while the propellant grade with TCP doesn't appear to self-deflagrate; rather it appears to thermally decompose.

The data (Table VIII @ 500 psi and 100g; Table IX @ 500 psi & 0g) indicate that binder thickness apparently has little observable effect upon burning rates of AP/PBAA sandwich burners. This result is in agreement with the data of Jones and Strahle (26).

The flames for all the 200 psi, 0g runs were laminar in nature. In the acceleration runs at 200 psi some flame turbulence was noted as a flickering of the flame from side to side. It was also observed from the increased width at the bottom of the burn profile that there was a tendency for the molten binder to be forced by the acceleration out past the binder AP interface and onto the AP. Binder flow onto the AP at +1 g conditions has been reported by Varney (17) and Jones and Strahle (26). It is believed that the flame flickering seen in the +100 g runs at 200 psi was caused by small pockets of oxidizer rich gases being liberated under the molten binder by thermal decomposition of the AP. This acceleration induced binder flow evidently quenches AP decomposition.

At pressures of 500 psi and 800 psi all flames were turbulent in appearance regardless of the acceleration field. In the case of the ultra high purity AP runs, this is attributed to the self-deflagration

of the AP (see section IV C). In the case of the propellant grade AP it is believed that the flame liberates sufficient heat to thermally decompose the AP above the primary flame zone. This decomposed oxidizer then flows outward from the wafer face, creating a turbulent flame.

A successful burn for the propellant grade AP (with TCP) sandwiches burned at 800 psi and 100 g was not obtained. All attempts met with either unsuccessful ignition, or the flame being extinguished within one-tenth inch of burn.

From Table VIII it is observed that AP/PBAA sandwich burners made with ultra high purity polycrystalline AP wafers exhibit burning rate acceleration sensitivity. Below the P_{d1} or pure AP, average burning rate decreased with increasing acceleration. Above P_{d1} of pure AP, average burning rate increased with increasing acceleration. Sandwiches made with propellant grade AP with TCP additive showed no significant augmentation in average burning rate for acceleration conditions.

These results indicate that burning rate acceleration sensitivity of nonmetallized composite propellants is due in part to the interaction of the binder melt with the self-deflagrating AP. For pressures below the P_{d1} of AP (approximately 300 psi for pure AP and apparently greater than 800 psi for propellant grade AP with TCP), acceleration induced binder flow onto the AP generally inhibits AP decomposition and the average burning rate decreases or remains unchanged. For pressures above the P_{d1} or AP, acceleration induced binder flow appears to affect the burning rate as a result of mixing of the binder melt with the deflagrating AP/AP melt. The higher the pressure, the higher the binder "post" and the greater the

binder/AP interaction (puddling, etc., see Figures 24 and 25). This could affect both heterogeneous and gas phase reaction rates. The average burning rate augmentations at 100 g of approximately ten percent at 500 psi and 800 psi (see Table VIII) are also in general agreement with propellant augmentation data (3, 15).

As indicated above, the burning rates reported in Tables VIII, IX, and X are average burning rates. To obtain an estimate for the transient behavior of the burning rate, the increment of burn time over which the data were taken was split into two equal parts for 100 g and 0 g runs. This was done for ultra high purity AP/PBAA sandwich runs which were made at 500 psi and 800 psi. The data are summarized in Table XI. It was found that the burning rates at 0 g for both pressures increased between increments while those at 100 g decreased. At 500 psi the second increment average burning rate at 0 g did not exceed the second increment average burning rate at 100 g. At 800 psi the average burning rate of the second increment for the 100 g run was lower than the second increment average burning rate of 0 g run. These results indicate the complexity involved in modelling the mechanism(s) for acceleration induced burning rate augmentation of sandwich burners and/or nonmetallized composite propellants. The deflagration rate of pure AP at pressures above its P_{dl} increases with pressure. As a consequence, the amount of binder not consumed is greater in the 800 psi runs than in the 500 psi runs. Apparently a small amount of binder overflow onto the AP enhances the average burning rate (17, 26) of the sandwich. If excess binder builds up on the surface of the AP, it is possible that it acts as a heat sink and quenches the reaction.

The effect of preferred interfacial reactions between the binder and the AP was briefly considered. A sandwich was constructed in which only one AP wafer was cured to the binder. A matching AP wafer was placed firmly against the cured binder to form a sandwich. This sandwich burner was identical to the normal burner except one side was "dewetted", i.e., it had a significantly different AP/binder interfacial condition on one side. This configuration should bias the reaction front to interfacial reactions. A test was conducted with this sandwich at 500 psi and 0 g. No large order preferential burning down the unbonded interface was observed in the motion picture. However, it appeared that the unbonded AP wafer was consumed at a slightly faster rate than the bonded wafer. In addition, the average burning rate for this sandwich was significantly greater than that obtained when both AP wafers were bonded to the PBAA (Table IX). Additional tests will be required to clarify the significance of this result.

Although the measurements for burning rate calculations were taken from a projected image with a vernier caliper to within a thousandth inch, the uncertainty of the exact location of the nadir of the burn makes the reported third place accuracy questionable.

C. Schlieren Study of Sandwich Combustion

Several motion picture and extinguishment studies of sandwich burners have been conducted (17, 26, 28). These studies have visually depicted the effects of various operating conditions (such as pressure, type and quantity of catalyst, and etc.) on the burning surface and flame configurations. To obtain additional information on the flame structure it is necessary to use a technique which will give information on density or temperature variations within the combustion zone. In addition, the deflagration of AP is not visible at nominal pressures (< 1000 psi).

Any interaction of the AP deflagration or decomposition products with the visible flame is not directly obtained by visual observation. Therefore, a combustion bomb was designed and fabricated which could be utilized for various optical studies (schlieren, holograms, etc.) of burning propellants.

The objective was to try to simulate on a large two-dimensional scale the interface between the ammonium perchlorate and binder of a simple composite propellant in order to gain visual information about how it burns in various environments (i.e., whether the type of flame is laminar, turbulent, premixed, diffusive, or a combination of some or all). The type of flame(s) that exists has a dominant role in any combustion modeling.

As a preliminary to what was observed, a brief summary of some results already obtained for AP sandwiches with PBAA binder (17, 19, 26) is presented:

1. Melted PBAA flows over some of the AP, the amount of AP covered by binder melt being dependent on pressure.
2. The binder-oxidizer interface is smooth, i.e., there are no significant interfacial reactions.
3. The maximum surface regression occurs in the AP in the pressure range from AP deflagration limit (approximately 300 psi) to 1000 psi.
4. At a binder thickness somewhere below 50 microns a "hump of AP" (covered with molten binder) can occur and gives asymmetrical burning (19).
5. A liquid layer is present on the AP during combustion at pressures above the lower deflagration limit.

The discussion below is based upon examination of the color films on a large screen. The color prints* included in the report are representative of the data obtained but lack the clarity of the original films.

Figure 26 is a color print from the film taken at 800 psi. Three things in particular are of note. The exposed binder has a large height (which results from the high deflagration rate of AP at 800 psi) and the flame color (both the primary flame coming from the surface and that on the binder) is yellow. The orange colors coming off of the binder at lower pressures (discussed below) are absent. A large amount of visible smoke is also observed.

Figure 27 is a color print from the schlieren film taken at 800 psi. It may be characterized by the gross "turbulence" visible at heights above the primary flame, a general darkening of colors from AP smoke interaction, and the long dark center area from the exposed binder. Particularly interesting are the light green, orange, and orange-reds in the primary flame on both sides of the binder.

Figure 28 is a color print from the film taken at 500 psi. Binder protrusion above the AP is less than at 800 psi. There is also less visible smoke from the AP than at 800 psi. The appearance of a large amount of orange in the binder flame and a lesser amount being present in the primary flame means that a red schlieren color shift interacting with yellow flame light can no longer be positively distinguished.

Figure 29 is a color print from the schlieren film taken at 500 psi. "Turbulence," while still severe, has decreased. In Figure 29 the presence

*Except for a few specially prepared copies of this report, only black and white reproductions are presented.

of light green color along the side of the primary flame is of primary importance since the oranges present could be from flame light. The only way to obtain the green is from a blue schlieren light shift interacting with the yellow flame.

Figure 30 is a color print from the film taken at 200 psi. This pressure was below the low pressure deflagration limit (P_{dl}) for AP. The AP protrudes above and slopes away from the flame zone.

Figure 31 is a color print from the schlieren film taken at 200 psi and is markedly different from those taken at 500 and 800 psi. Gas flow above the sandwich is essentially laminar with some mixing with the N_2 purge gas. No green is visible along the primary flame. Dark regions exist on each side above the decomposing AP.

Figure 32 is a color print from the film taken at 100 psi. It is similar to Figure 30 except that the ability to distinguish between a primary flame and a binder flame has been lost, and the area encompassed by the flame (both height and width) is reduced.

Figure 33 is a color print from the schlieren film taken at 100 psi. The gas flow is quite laminar and again the absence of any green in the flame may be noted. The dark regions observed at 200 psi are more dominant. Figure 34 is a color print from the schlieren film taken at 100 psi with the blue-red color matrix positioned horizontally to indicate density gradients normal to the original burning surface.

Figure 35 is a color print from the film taken at 500 psi. It is different from the other photographs (schlieren and non-schlieren) in that the sandwich faces were not parallel to the optical axis of the schlieren system. The purpose of having the angled orientation

was to give a representation of the averaging effects that must be considered in any interpretation of Figures 26 through 34. Sandwich height varied from .3 to .45 inch but a special emphasis was placed on consistency of width (.15 inch) in order to avoid having to consider different averaging effects at the various pressures employed.

At 500 and 800 psi there is evidence (green color resulting from the blue schlieren light shift and the bright yellow flame) of a very low density area along the side of the primary flame. This indicates the probable existence of a diffusion flame. The gases evolving from the surface (both from the primary flame and the deflagrating AP) appear to be turbulent. However, the averaging effect may bias the schlieren. To verify this, additional schlieren will have to be taken with less sandwich depth in the optical path and with slightly increased magnification on the film plane.

The lack of any green in the schlieren pictures at 200 and 100 psi indicates a possible change in the burning process has occurred. The 100 psi schlieren pictures indicate that the AP pyrolysis products evolving from the near-vertical AP surfaces continue to react for some distance above the visible flame. The gases evolving from the surface (including the AP decomposition) are visibly laminar. The dark regions which exist on either side of the primary flame above the AP are thought to result from the opaque AP decomposition gases.

The significant differences in the results obtained at high and low pressures are presumed to result from operation above and below the lower deflagration limit of AP. Schlieren films taken just above and below the P_{dl} will be required to clarify this behavior.

It should also be mentioned that the "fingerlike flamelets" noted by Boggs (28), for carboxyl terminated polybutadiene, hydroxyl terminated polybutadiene and polyurethane binders were present for the polybutadiene acrylic acid binder used in this investigation (Fig. 35)

Either laser schlieren or laser interferometry pictures would eliminate any possibility of flame light interaction through use of suitable filters and should be taken for substantiating and extending these initial findings.

D. A Study of Preferential Interfacial

Reactions and Surface Accumulation Effects

D.1 Introduction

To investigate the presence of preferential interfacial reactions and their possible affect upon burning rate acceleration sensitivity four nonmetallized solid propellants were selected. Each had a different oxidizer particle (ammonium perchlorate) size distribution and similar binder characteristics. Propellant designations and properties are given in Table IV. Each propellant was tested in a pre-stressed (dewetted) and unstressed (as-cast) condition. Propellant strands were burned in positive, negative and static (zero g) acceleration environments.

Comparison of each propellant with only the interfacial characteristics modified was then made to determine if preferential interfacial reactions existed.

D.2 Results for Propellant B-1

Tests were first conducted to insure that the $\frac{1}{2}$ in. by $\frac{1}{2}$ in. strand burners yielded burning rates in agreement with the NASA data. The results are presented in Figure 36 and indicate good agreement.

In order to determine whether surface accumulations (of melts, impurities, etc.) were of significance in the burning rate augmentation, strand cross-sectional area and length were varied. The data in Table XII indicate that to strand cross-sections of 1 inch x 1 inch, surface area had only a small effect on augmentation. Figure 37 shows the effect of burn time (strand length) on augmentation. The NPS data indicate that at 1000 g only small variations in burning rate occurred with time. At 250 g, an initially constant burning rate is seen to increase with time. Also shown in Figure 37 are Northam's results for the same propellant (16). Northam's data were obtained at 600 psia whereas the NPS data were obtained at 500 psia. However, this difference will not significantly alter the comparison. The most significant difference between the LRC and NPS tests was the burning surface area. The NPS data was obtained from $\frac{1}{2}$ inch x $\frac{1}{2}$ inch cross-section strands and the LRC data was obtained from 2.7 inch x 5.4 inch slabs. Figure 37 indicates that the slab burning rate augments significantly more than the strand burning rate and exhibits significantly greater transient phenomena. These results suggest the existence of large scale surface effects and will be discussed below.

Burning rate data obtained for propellant B-1 in positive and negative acceleration fields are presented in Figure 38. The base burning rate (\dot{r}_0) and augmentation of both the pre-stressed and unstressed propellants were essentially the same. Augmentation obtained at a negative 1000g was 0.93 in both the dewetted and as-cast conditions. Considerable data scatter was encountered in a high positive acceleration environment while negative acceleration data scatter was negligible. The LRC datum point in Figure 38 was taken from Reference 16.

Northam extinguished B-1 propellant slabs in acceleration environments and found large scale surface pitting (16). The size of the surface pitting was of the same order as the size of the $\frac{1}{2}$ inch x $\frac{1}{2}$ inch strand cross-sections employed in this investigation. Small particles of unidentified material were found in some of the pits. Thus, Northam has concluded that the observed large augmentation resulted primarily from surface accumulation of an impurity or propellant additive (tricalcium phosphate (TCP), etc.).

The above results (16) may explain the wide spread in the strand data at high accelerations (Figure 38), the difference in the transient burning results shown in Figure 37 and the two rather distinct groupings of data at 250 g and 500 g (Figure 38). At times the strand surface is the equivalent of a pit bottom and at times not. However, in the numerous tests conducted, negligible augmentations were never obtained at high accelerations as might be expected if the burning were ever on the equivalent of a plateau. In addition, acceleration sensitivity has been reported for nonmetalized propellants that did not contain any TCP or carbon (1). Spinning motor data (10) have also shown that for some nonmetalized composite propellants, no transient burning rates in acceleration environments exist. These results suggest that two augmentation mechanisms may exist. The dominant mechanism for the AP/PBAA propellant used in this study was obviously the surface accumulation of solid material(s).

D.3 Results for Propellant B-2

Figure 39 presents the burning rate augmentation data obtained with the B-2 propellant for both the pre-stressed and unstressed conditions.

Base burning rates were essentially the same for the dewetted and as-cast propellants. Augmentation at negative accelerations was slightly less than one for the as-cast propellant. A five percent augmentation resulted in the negative 50 g acceleration field for the dewetted propellant.

Considerable data scatter was present in the positive g environments. Fast burns were especially prevalent for the dewetted propellant at 50 and 250 g. Negative acceleration data showed very little scatter.

Pre-stressed propellant data scatter may have been due to internal fracture of the propellant. This propellant was stressed very close to fracture to attain dewetting. Data scatter could also have been caused by inhomogeneity of the propellant mix. Propellant B-2 was made in a small batch with the possibility of settling of the oxidizer particles during cure.

D.4 Results for Propellant N-3

Augmentation data for propellant N-3 in both the pre-stressed and unstressed conditions are presented in Figure 40. Base burning rates and augmentation were essentially the same for both dewetted and as-cast propellants. Augmentation at negative accelerations was negligible. Data scatter was prevalent for the pre-stressed propellant tests conducted in a positive acceleration field. This scatter may have been due to small batch size and internal fracture.

D.5 Discussion

Both propellant B-2 (AP/PBAA) and propellant N-3 (AP/PBAN) were somewhat translucent and did not contain any additives (carbon, etc.)

to prevent radiative heat transfer below the surface during combustion. Substantial subsurface heating may have been occurring which could have softened or altered the binder characteristics. The positive acceleration environments may then have varied effects upon the propellant, yielding the observed data scatter. Burning rate data scatter in acceleration environments are typically greater for nonmetallized propellants that do not contain opacifiers than for nonmetallized propellants that include such additives or for metallized composite propellants (1,2,3.).

Table XIII presents a summary of general trends noted for each propellant tested.

Base burning rate was essentially unchanged for all propellants when dewetted. For the preferential interfacial reaction (PIR) model (3) to explain this observed base burning rate data, one of the following arguments could be made:

1. No dewetting had occurred to the propellants when stressed.
2. Large dewetted oxidizer particles in the pre-stressed strands had no effect on the base burning rate.
3. Large dewetted oxidizer particles were "blown" off the surface in a zero g condition. However, a combustible pit was left by the oxidizer particle. The increased burning area of the pit offset the energy lost by the oxidizer depletion, resulting in no appreciable burning rate change.

It is unlikely that no dewetting occurred since considerable data support the presence of dewetting in all the stressed propellants.

The positive acceleration data was meaningful for propellant B-1. However, data scatter was too great for positive acceleration tests with propellants B-2 and N-3 to consider that data in more than a qualitative manner. The augmentation obtained for the dewetted B-1 propellant did not change significantly from the "as cast" data. Either argument 2 or 3 above could be used to explain this observation in light of the PIR model.

It should be noted that the data obtained in positive acceleration environments for propellant N-3 are inconsistent with Sturm's original model (3). The original model assumed large oxidizer particles did not contribute to burning rate augmentation. Propellant N-3 consisted of a narrow cut (420-500 micron) of large oxidizer particles. Yet, this propellant exhibited burning rate augmentation in both the pre-stressed and unstressed conditions.

Assuming preferential interfacial reactions do exist, no augmentation should have resulted in a negative g acceleration field unless physical extraction of the oxidizer particles had taken place. If oxidizer particles were extracted, the burning rate may have increased, decreased or remained the same as the base burning rate. This would be dependent on the condition of the pit remaining after particle extraction. If the resultant pit was combustible, the burning rate could increase due to increased burning area. If the pit was combustible and the burning area of the pits off-set the depletion of oxidizer, no change in burning rate would result. If the pit was inert (fuel rich), the burning rate would decrease due to oxidizer depletion.

All propellants tested exhibited a decrease in burning rate in the unstressed condition at all negative accelerations. The data were most significant for propellant B-1. If preferential interfacial reactions were to explain this phenomenon, physical extraction of oxidizer particles had to have taken place. The resulting pits left by the extracted particles had to be inert or the AP lost to combustion had a greater effect than the increased active surface area. Operating on this assumption, stressing the propellants should have resulted in more large oxidizer particles being extracted and a larger decrease in burning rate. However, the pre-stressed B-1 propellant had the same augmentation at negative 1000 g as the unstressed propellant. This behavior cannot be readily explained with the model.

The data for propellant B-2 (Figure 39) show an increase in burning rate for the pre-stressed propellant at negative accelerations. For this to have occurred within the framework of the PIR model, pits remaining after oxidizer extraction had to be combustible and had to more than compensate for the AP lost to combustion. This contradicts the assumptions made to justify the unstressed propellant data and is another inconsistency not readily explained by the model.

The N-3 data further verify the model inconsistencies found for propellant B-2.

The propellants that had soft binders (B-2 and N-3) exhibited burning instabilities and self extinguishment in high positive acceleration fields (Table XIII). Post-fire propellant residue remaining in the rigid inhibitors was subsequently burned in an atmospheric environment

after removal from the case. These burning instabilities imply that some physical interaction of the binder and oxidizer occurs at the higher positive accelerations. Possibly the oxidizer particles were forced down into the soft binder causing partial or complete extinguishment. This suggests another possible mechanism for burning rate acceleration sensitivity.

V. CONCLUSIONS

A. Ammonium Perchlorate Deflagration

- 1) Initial crystal size used in pressed AP pellets does not significantly affect the burning rate when high molding pressures (30,000 psi) are used.
- 2) Surface melt exists during AP deflagration. The quantity of melt may depend upon the ignition energy (or flame zone location, etc. in propellant combustion) and surface configuration.
- 3) The burning rate acceleration sensitivity of AP is opposite to that normally observed for nonmetallized composite propellants (i.e. AP burning rate decreases and deflagration extinguishment eventually occurs with increasing acceleration directed normal and into the burning surface). Therefore, AP deflagration by itself cannot be used to explain the acceleration sensitivity of these propellants.
- 4) Impurities such as tricalcium phosphate and sulfated ash substantially increase the effective low pressure deflagration limit of AP.

B. AP/PBAA Sandwich Burners

- 1) Binder thickness apparently has little effect upon burning rates (for thicknesses greater than 100 μ).
- 2) AP/PBAA sandwich burners made with ultra high purity polycrystalline AP wafers exhibit burning rate acceleration sensitivity.

- 3) For pressures below the P_{dl} of AP (approximately 300 psi for pure AP and apparently greater than 800 psi for propellant grade AP with TCP and sulfated ash), acceleration induced binder flow onto the AP inhibits AP decomposition and the average burning rate decreases or remains constant.
- 4) For pressures above the P_{dl} of AP, acceleration induced binder flow appears to affect the burning rate by mixing of the binder melt with the deflagrating AP/AP melt.
- 5) A small amount of binder flow onto the AP apparently enhances the average burning rate. If excess binder builds up upon the AP surface it quenches the reaction.
- 6) AP/PBAA sandwich burning rates increase with time at 0 g and decrease with time at 100 g. The higher the pressure, the more pronounced the effect. Future tests should include measurement of the time dependent burning rates throughout the entire burn.
- 7) Schlieren studies indicate the complexity of the interaction of the AP deflagration (or pyrolysis) products with the binder pyrolysis and primary flame products. Flame structure appears to be different for pressures above and below the low pressure deflagration limit of AP.
- 8) Sandwich burner flames below the P_{dl} of AP are laminar. Above the P_{dl} the flames appear to be turbulent but further tests will be required to verify this result.

- 9) Two distinct flame regions were observed, one above the binder (or binder post) and one near the binder/AP interface. Both flames were non-steady and consisted of many small "flamelets."

C. Propellants

- 1) Inconsistencies between the basic assumption of preferential interfacial reactions in Sturm's model (3) and observed phenomena coupled with previous evidence (19) leads to the conclusion that preferential interfacial reactions are not responsible for the burning rate acceleration sensitivity of nonmetallized AP/PBAA composite propellants. Significant preferential interfacial reactions did not exist for the propellants investigated at the pressures and acceleration levels in which they were tested.
- 2) Any solid material additive (carbon, tricalcium phosphate, or impurity) may result in pitting and burning rate augmentation in an acceleration environment, but an additional mechanism(s) is also present which results in augmentation.
- 3) Burning rate acceleration sensitivity of nonmetallized composite propellants is due in part to the interaction of the binder melt with the deflagrating AP/AP melt.
- 4) Propellants with "soft" binders burn unstably and may extinguish in a high acceleration environment. This may be due to physical interactions of the oxidizer and binder.
- 5) Nonmetallized composite propellants that do not incorporate opacifiers to prevent subsurface heating appear to burn more erratically in positive acceleration environments.

VI. REFERENCES

1. Netzer, D. W. et. al, "An Investigation of the Effects of Acceleration on the Burning Rates of Solid Propellants," Naval Postgraduate School Report NPS 57NT9101A, 1 Oct 1969.
2. Anderson, J. B. and Reichenbach, R. E., "An Investigation of the Effect of Acceleration on the Burning Rate of Composite Proepllants," Naval Postgraduate School Report NPS 57RV7071A, 28 July 1967.
3. Sturm, E. J. and Reichenbach, R. E., "A Study of the Burning Rates of Composite Solid Propellants in Acceleration Fields," Naval Postgraduate School Report NPS 57RV8121A, 5 Dec 1968.
4. Pinney, C. A., "Cinematographic Study of Composite Solid Propellant Combustion in Positive and Negative Acceleration Fields," M. S. Thesis Naval Postgraduate School, Dec 1970.
5. Broddner, S., "Effects of High Spin on the Internal Ballistics of a Solid Rocket Motor," Astronautica Acta, Vol 15, p. 191-197, 1970.
6. Nagaoka, T , Ito, K., and Koreki, T., "Combustion of Propellant Under Spin Acceleration," 8th International Symposium on Space Technology and Science, Tokyo, Japan, AGNE Publications, Inc., 1969.
7. Northam, G. B. and Jessee, W. P., "Experimental Investigation of the Effect of Aluminum size and Loading on the Burning Rate of Solid Propellants Under Acceleration ," NASA TN D-5397 , Sept 1969.
8. Cowles, D. E., Schroeder, Jr., R. C. and Netzer, D. W., "The Effect of Acceleration on Composite Propellant Combustion," Naval Postgraduate School Report NPS-57NT70091A, 1 Sept 1970.
9. King, M. K. and McHale, E. T., "An Optical Bomb Study of the Combustion of Solid Propellants in High Acceleration Fields," Atlantic Research Corporation, Second Annual Technical Report, 1969.
10. Willoughby, P. G , et. al, "Investigation of Internal Ballistic Effects in Spinning Solid Propellant Motors," United Technology Center Report UTC 2281-FR, Oct 1968.
11. "Investigation of Particle Growth and Ballistic Effects on Solid Propellant Rockets," United Technology Center Report UTC 2128-FR, June 1966.
12. Glick, R. L., "An Analytical Study of the Effects of Radial Acceleration Upon the Combustion Mechanism of Solid Propellant," Contract NAS7-406, NASA Report No. 66218, Thiokol Report No. 42-66, 1966.

13. Glick, R L., "Comment on an Investigation of the Acceleration Induced Burning Rate Increase of Nonmetalized Composite Propellants," AIAA Journal, 9, No. 3, p. 542.
14. Iwanciw, B. L., et. al., "The Effect of Acceleration on Solid Composite Propellant Combustion," AIAA Preprint No. 64-227, June 1964.
15. Cowles, D. and Netzer, D., "The Effect of Acceleration on Composite Propellant Combustion," Comb. Sci. and Tech., Vol 3, pp 215-229, 1971.
16. Northam, G. B., "The Effects of Some Propellant Composition Variables on Acceleration Induced Burning-Rate Augmentation of Solid Propellants," Presented at 1971 JANNAF Combined Propulsion Meeting, Las Vegas, Nevada, Nov 1971.
17. Varney, M. A., "An Experimental Investigation of the Burning Mechanisms of Ammonium Perchlorate Composite Solid Propellants," PhD Thesis, Georgia Institute of Technology, May 1970.
18. Boggs, T. L., Derr, R. L., and Beckstead, M. W., 1968, "Surface Structure of Ammonium Perchlorate Composite Propellants," AIAA Journal. Vol 8, No. 2.
19. Hightower, J. D. and Price, E. W., "Experimental Studies Relating to the Combustion Mechanism of Composite Propellants," Astronautica Acta, Vol 14, 1968.
20. Northam, G. B., "Acceleration-Induced Transient Burning-Rate Augmentation of an Aluminized Solid Rocket Propellant," Phd Thesis, Virginia Polytechnic Institute, 1969.
21. Willoughby, P. G., Baker, K. L., and Hermsen, R. W., "Photographic Study of Solid Propellants Burning in an Acceleration Environment," UTC Contractor Report for NASA, NASA CR-66824.
22. Willoughby, P. G., Baker, K. L., and Hermsen, R. W., "Photographic Study of Solid Propellants Burning in an Acceleration Environment," 13th Symposium (International) on Combustion, pp 1033-1045.
23. Willoughby, P. G., Crowe, C. T , and Baker, K. L , "A Photographic and Analytical Study of Composite Propellant Combustion in an Acceleration Field," Journal of Spacecraft and Rockets, Vol 8, No. 4.
24. Guirao, C. and Williams, F. A., "A Model for Ammonium Perchlorate Deflagration between 20 and 100 atm., AIAA Journal Vol 9, No. 7, July 1971, pp 1345-1356.
25. Varney, A. M. and Strahle, W. C., "A Two Dimensional Sandwich Burning Study of AP Oxidizer With Four Propellant Binders" 7th JANNAF Combustion Meeting, CPIA Pub. No 204, Vol 1, p. 153.

26. Jones, H. E. and Strahle, W. C., "A Motion Picture Study of AP Sandwich Combustion," 8th JANNAF Combustion Meeting, CPIA Pub. No 220, Vol 1, p. 95
27. Boggs, T. L., Price, E. W., and Zurn, D. E., "The Deflagration of Pure and Isomorphously Doped Ammonium Perchlorate," 13th Symposium (International) on Combustion, p. 995.
28. Boggs, T. L. and Zurn, D. E., "The Deflagration of Ammonium-Perchlorate -- Polymeric Binder Sandwich Models," 8th JANNAF Combustion Meeting, CPIA Pub No 220, Vol. 1
29. Northam, G. B., "Effects of the Acceleration Vector on Transient Burning Rate of Aluminized Solid Propellant," J. Spacecraft, Vol 8, No. 11, Nov. 1971, p. 1133.
30. Boggs, T. L., "Deflagration Rate, Surface Structure, and Subsurface Profile of Self-Deflagrating Single Crystals of Ammonium Perchlorate" AIAA Journal, vol 8, No. 5, May 1970, p. 867.
31. Derr, R. L. and Boggs, T. L., "Role of Scanning Electron Microscopy in the Study of Solid Propellant Combustion: Part III. The Surface Structure and Profile Characteristics of Burning Composite Solid Propellants," Comb. Sci. & Tech., vol 1, 1970, p. 369.
32. Boggs, T. L. and Kraeutle, K. J., "Role of the Scanning Electron Microscope in the Study of Solid Rocket Combustion, I. Ammonium Perchlorate Decomposition and Deflagration," Comb. Sci. & Tech., Vol 1, 1969, p. 75.
33. Hightower, J. D. and Price, E. W., "Two-Dimensional Experimental Studies of the Combustion Zone of Composite Propellants," 2nd ICRPG Combustion Conference, CPIA Pub No. 105, vol 1, p 421.
34. Shannon, L. J. and Peterson, E. E., "Burning Velocity of Ammonium Perchlorate Strands and Crystals" AIAA Journal, Vol 6, No 8, p 1594.
35. Wood, J. E., Ph.D. Thesis, Naval Postgraduate School, Monterey, Calif., 1972 (to be published).
36. Lindsey, G. H. and Wood, J. E., "An Isotropic Theory for Dewettable Solids," Naval Postgraduate School Report No. NPS-57Li71011A, 31 Jan. 1971.

Table I Summary of Observed Behavior in Acceleration Environments
for Nonmetallized Composite Propellants

PRESSURE:	No consistent trend, increasing pressure increases or decreases \dot{r}/\dot{r}_0	(1,2,3)
TEMPERATURE:	\dot{r}/\dot{r}_0 increases slightly with increasing temperature for high g (>300g)	(1,3)
BURNING RATE:	\dot{r}/\dot{r}_0 increases with decreasing \dot{r}_0	(1,3)
AP CRYSTAL SIZE:	No significant effect at high g	(1)
	No consistent results at low g	(1)
SURFACE AREA:	No appreciable effect	(1)
METAL CONTENT:	Increasing % Al increases \dot{r}/\dot{r}_0 below 150g	(2,7)
	Increasing % Al increases or decreases \dot{r}/\dot{r}_0 above 150g	(1,2,7,10)
BINDER TYPE:	PU, PBAN, PBAA, and CTPB exhibit different behavior in acceleration environments. PU-AP extinguishes at high g. PBAN-large AP does not burn at high g.	(1,2,9)
BURN TIME:	Very small, if any, time effects	(1,3,10)
MAGNITUDE & DIRECTION OF ACCELERATION:	0g to 150g threshold acceleration below which $\dot{r}/\dot{r}_0 = 1$ Above threshold acceleration, \dot{r}/\dot{r}_0 increases with increasing +g. At high +g, \dot{r}/\dot{r}_0 increases more slowly and in some cases approaches a constant value Small changes in \dot{r}/\dot{r}_0 observed for -g No change in \dot{r}/\dot{r}_0 for g directed parallel to surface No evidence of AP leaving surface at 0, <u>+107g</u>	(1,2,3,6,10) (1,2,3,5,7,10) (1,2,3,5) (3,8,9,15) (14) (4,8)
MEASURED BURNING RATE:	Significant scatter in data and varying behavior to approximately 200g	(1,2,3)

Table II Proposed Models and/or Mechanisms For Acceleration Sensitivity of Nonmetallized Composite Propellants

<p>Modified granular diffusion flame (12) (Effect of acceleration on gas phase combustion)</p>	<p>Many inconsistencies between model predictions and observed experimental behavior (2,8,9,12,15)</p>
<p>Flame, free AP (3,13)</p>	<p>Adequately explains most observed behavior (1,3) No direct experimental confirmation (8,15) Much evidence against basic assumption of preferential interfacial reactions (17,18,19)</p>
<p>Surface melt(s) interaction (8,15)</p>	<p>No direct experimental confirmation (8,15)</p>

Table III AP Specifications

<u>Designation</u>	<u>Crystal Size</u>	<u>Principal Impurities (wt%)</u>
UHP (ultra high purity)	38.1 % > 297 μ 81.9 % > 211 μ 99.6 % > 104 μ	Sulfated Ash 0.01%
Propellant Grade (regular 200 μ rounded)	* { 3-11% > 279 μ 24-52% > 211 μ 85-96% > 104 μ	{ Na and K 0.03% Ash 0.06% Chlorides 0.05%
Propellant Grade with conditioner (regular 200 μ rounded)	* { 3-11% > 297 μ 13-43% > 211 μ 85-98% > 104 μ	{ Chlorides 0.07% Sulfated Ash 0.40% Tricalcium Phosphate 0.20%

*typical values from manufacturer data sheet

Table IV Propellant Specifications

<u>Designation</u>	<u>Binder (Ingredients and wt %)</u>	<u>AP (size & wt %)</u>	<u>Additives (wt%)</u>	<u>Manufacturer</u>
B-1	PBAA-HA 14.52% ERL-2795 2.11%	UNG 188 μ , 54.06% GND 26 μ , 29.11% (with TCP)	Thermax 0.20%	NASA Langley Research Center
B-2	PBAA-HA 21% ERL 2795 4%	UNG-Rounded 200 μ , 56.25% GND 18 μ , 18.75% (with TCP)	none	Thiokol Chemical, Huntsville
N-1	PBAN 21%	8.8 μ - 79%	none	NWC, China Lake
N-3	PBAN 21%	420-500 μ - 79%	none	NWC, China Lake

Table V
Pure AP Pellet Results

Burning rate in/sec	Acceleration, g	Pressure (psia)	Ignition Method*	Observation
.180	0	500	BP+W	No inhibitor, method unreliable-many fast burns
.181	0	500	BP+W	Mold time 24 hr., powdered AP
.180	0	500	BP+W	Mold time 24 hr., powdered AP
.176	0	500	BP+W	
.179	0	500	BP+W	
.177	0	500	BP+W	
.178	0	500	BP+W	
.177	0	500	BP+W	
.178	0	500	BP+W	
.183	0	500	BP+W	
.175	44	500	BP+W	2 or 3 AP spheres (~.010 in) post fire residue
.175	48	500	BP+W	
.159	49	500	BP+W	
.164	50	500	BP+W	
.151(?)	100	500	BP+W	2 or 3 AP spheres (~.010 in) post fire residue
.170	94	500	BP+W	
.163	99	500	BP+W	
.173	100	500	BP+W	
.132(?)	249	500	BP+W	unburned AP in bottom
.148	255	500	BP+W	
.144(?)	255	500	BP+W	
.153	249	500	BP+W	

Table V (Cont'd)
 Pure AP Pellet Results


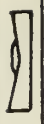


<u>Burning rate</u> <u>in./sec</u>	<u>Acceleration,</u> <u>g</u>	<u>Pressure</u> <u>(psia)</u>	<u>Ignition</u> <u>Method*</u>	<u>Observation</u>
no burn	500	500	BP+W	slight pitting of surface
no burn	500	500	BP+W	
no burn	478	500	BP+W	
no burn	497	500	BP+W	
no burn	500	500	BP+W	
no burn	500	500	BP+W	before  after 
no burn	500	500	BP+W	before  after 
.167	-472	500	BP+W	
.178	-497	500	BP+W	
.179	-500	500	BP+W	
no burn	0	295	BP+W	
no burn	0	325	BP+W	
.134	0	400	BP+W	
.139	0	400	BP+W	
.139	0	400	BP+W	
.210	0	600	BP+W	
.216	0	600	BP+W	
.246	0	700	BP+W	
.246	0	700	BP+W	
.276	0	800	BP+W	
.278	0	800	BP+W	

Table V (Cont'd)

Pure AP Pellet Results

<u>Burning rate</u> <u>in/sec</u>	<u>Acceleration,</u> <u>g</u>	<u>Pressure</u> <u>(psia)</u>	<u>Ignition</u> <u>Method</u>	<u>Observation</u>
.116(?)	0	500	W	
.138(?)	0	500	W	
.126(?)	0	500	W	
.110(?)	0	500	W	
.176	101	500	W	
.171	97	500	W	
.142	494	500	W	unburned AP in bottom
.173	494	500	W	a little unburned AP in bottom
.182	501	500	W	a little unburned AP in bottom
.134	481	500	W	
.148	494	500	W	

*BP+W: Black powder/glue/acetone and adjacent wire

W: Wire across face

Table VI Propellant Grade AP (with TCP) Pellet Results

<u>Burning rate in/sec</u>	<u>Acceleration, g</u>	<u>Pressure (psia)</u>	<u>Ignition Method</u>	<u>Observation</u>
no burn	0	500	BP+W	
no burn	0	500	BP+W	
no burn	0	500	BP+W	
no burn	1	500	BP+W	Mounted vertically
.036	0	500	BP+W	Very slow start
no burn	0	500	BP+W	Excess ignitor, surface severely pitted
no burn	0	500	BP+W	
no burn	0	500	W	
.043	0	500	W	
.096	1	500	BP/W	Thin layer of PMM on sides, mounted vertically, wire & ignitor directly on pellet
.078	1	500	BP/W	
no burn	45	500	BP+W	

Table VII Propellant Grade AP Pellet Results

<u>Burning rate in/sec</u>	<u>Acceleration, g</u>	<u>Pressure (psia)</u>	<u>Ignition Method</u>	<u>Observation</u>
.156/.118	0	500	BP+W	double burn out
.168/.112	0	500	BP+W	double burn out
.115 (?)	0	500	W	no burn 1st try
.114/.074(?)	0	500	W	double burn out

Table VIII

Summary of Data from AP(UHP)/PBAA Sandwich Tests

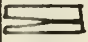
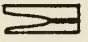


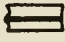
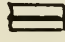

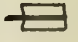
Pressure (psi)	Acceleration (g)	Average Burn Rate (in/sec)	Binder Thickness (in)	Burn Profile	Remarks
200	0	.07(9)	.003		Small laminar flame burning only in the vicinity of the binder AP interface. Some evidence of AP pyrolysis above the flame.
200	100	.06(4)	.003		Small flame burning only in the vicinity of the binder interface. Flame appeared to fluctuate more than the 200 psi, Og run. AP pyrolysis above the flame.
500	0	.17(7)	.006		Burned with wide nonsteady flame.
500	100	.20(9)	.003		Burned with wide nonsteady flame. Binder pools on the AP.
500	100	.19(5)	.003		Burned with wide nonsteady flame. Binder pools on the AP.
500	100	.20(2)	.007		Burned with wide nonsteady flame. No visible binder pooling on AP, however greater width of flame at binder AP interface suggests binder overflow onto AP.
800	0	.26(0)	.009		Burned with wide nonsteady flame. AP burned much faster than the binder, leaving an extended binder post. Large quantities of gray smoke from the AP observed.
800	100	.29(7)	.008		Burned with wide nonsteady flame. Binder was observed to puddle on both AP wafers. Large quantities of smoke from the AP observed.

Table IX

Summary of Data from AP(TCP)/PBAA Sandwich Tests

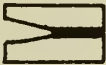
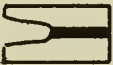


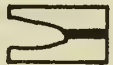
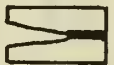
Pressure (psi)	Acceleration (g)	Average Burn Rate (in/sec)	Binder Thickness (in)	Burn Profile	Remarks
200	0	.08(9)	.002		Burned with a small laminar flame only in the vicinity of the AP/binder interface. Less evidence of AP pyrolysis than for the same run conditions with AP(UHP)
200	100	.08(4)	.003		Burned with a small nonsteady flame, burning occurred in the vicinity of the AP/binder interface. Binder appeared to puddle near the center of the sandwich and puddle remained during remainder of burn.
500	0	.12(7)	.002		Burned with nonsteady flame. It appeared that AP pyrolysis continued some distance above the flame zone.
500	0	.12(8)	.004		Burned with a nonsteady flame. AP pyrolysis continued for some distance above the flame zone.
500	100	.12(6)	.004		Burned with a nonsteady flame. Pyrolysis of the AP continued for some distance above the flame zone. No binder puddling was observed.
800	0	.18(9)	.002		Burned with a nonsteady flame. AP pyrolysis continued for some distance above the flame zone.
800	100	xxxxxx	xxxx		No successful runs for this condition.

Table X

Summary of Data from AP(UHP)/PBAA Single Bonded Face Sandwich Test

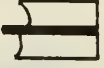
Pressure (psi)	Acceleration (g)	Average Burn Rate (in/sec)	Binder Thickness (in)	Burn Profile	Remarks
500	0	.19(9)	.003		Possibly a preferential consumption of the unbonded AP wafer. It appeared to decompose faster than the bonded wafer. Large quantity of gray smoke liberated from the surface of the AP. Burned with a wide nonsteady flame.

Table XI

Summary of Incremental Burning Rates for AP(UHP)/PBAA Sandwich Tests

Pressure (psi)	Acceleration (g)	First Increment Average Burn Rate (in/sec)	Second Increment Average Burn Rate (in/sec)	Average Burn Rate (in/sec)
500	0	.16(5)	.18(3)	.17(4)
500	100	.20(4)	.19(9)	.20(2)
800	0	.22(4)	.31(1)	.26(7)
800	100	.37(1)	.21(2)	.29(1)

Table XII

Effect of Strand Cross-section on Augmentation of Propellant B-1

Cross-section in x in	Augmentation \dot{r}/\dot{r}_0	Acceleration, g	
$\frac{1}{4} \times \frac{1}{4}$	1.12	247	
	1.06	247	
	1.06	251	
	1.04	249	
	1.11	251	
	1.08	248	
	1.11	250	
	1.14	992	
	1.14	1000	
	1.15	248	
	1.14	252	
$\frac{1}{2} \times \frac{1}{2}$	1.16	1000	
	1.17	1000	
	1.14	1000	
	1.16	996	
	1.17	996	
	1.17	1000	
	1.07	247	
	1.09	247	
	1 x 1	1.08	247
		1.08	247

(Strand length = 1 in., $\dot{r}_0 = .243$ in/sec)

Table XIII Summary of Data for As-Cast and Dewetted Propellants

Propellant	\dot{r}_{os}^* vs \dot{r}_o	Positive "G" Comparison	Negative "G" Augmentation, As-cast	Negative "G" Augmentation, Pre-stressed	Burning Rate Instabilities	Postfire Residue in Rigid Inhibitor
B-1	no change	stressed had slightly greater augmentation	.93 @ 1000g	.93 @ 1000g	no major	none
B-2	no change	stressed had slightly greater augmentation. large data scatter	.96 @ 50g .95 @ 1000g	1.05 @ 50g .99 @ 1000g	slow starts, erratic burns, plateaus 250 -- 1000g	unburned ** propellant, 500 -- 1000g
N-3	no change	stressed had slightly greater augmentation. large data scatter	.98 @ 250g	1.0 @ 250g	slow starts, plateau regions 100 -- 250g, no burn above 250g	unburned ** propellant, 250g

* \dot{r}_{os} : base burning rate, pre-stressed condition

\dot{r}_o : base burning rate, as-cast condition

**propellant burned in atmospheric environment after removal from case.

I. Determination of AP Effects on Burning Rate Acceleration Sensitivity

A. As-cast and pre-stressed (dewetted) strands

Strand size: $\frac{1}{2}$ in x $\frac{1}{2}$ in cross-section; length, $\frac{1}{4}$ -2 in.

Propellants: PBAA/AP, PBAN/AP

Pressure: 250 - 1000 psia

Acceleration: 0 to + 1000g

Data: \dot{r} vs g, \dot{r} vs length burned, \dot{r} vs surface area

B. AP pellets

Type: ultra high purity, propellant grade with and without TCP

Size: $\frac{1}{2}$ in. diameter x $\frac{1}{4}$ in. thick

Pressure: 300 - 800 psia

Acceleration: 0 to + 1000g

Data: \dot{r} vs g

II. Determination of Surface Melt Effects (AP & Binder)

Propellant Sandwiches

Ingredients: AP with and without TCP / PBAA

Pressure: 100 - 800 psia

Acceleration: 0 to + 100g

Data: High Speed Motion Pictures, Color Schlieren (zero g), burning rates, physical behavior, gas-phase combustion observation

A. CENTRIFUGE:

3 ft radius
0 to 1000g
0 to 1500 psi

Determine average burning rate

B. PHOTOGRAPHIC CENTRIFUGE

1 ft radius
0 to 110g
0 to 800 psi
100' Hycam camera

C. COMBUSTION BOMB

Nitrogen Purge
0 to 1000 psi
400' Hycam Camera for high speed motion pictures
and color schlieren

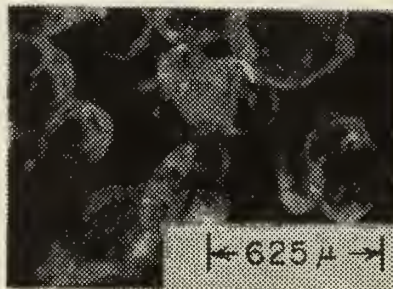
Figure 2 Experimental Apparatus



(a) Propellant Grade
with TCP



(b) Propellant Grade
without TCP



(c) Ultra High Purity

Figure 3 Photomicrographs of AP Crystals

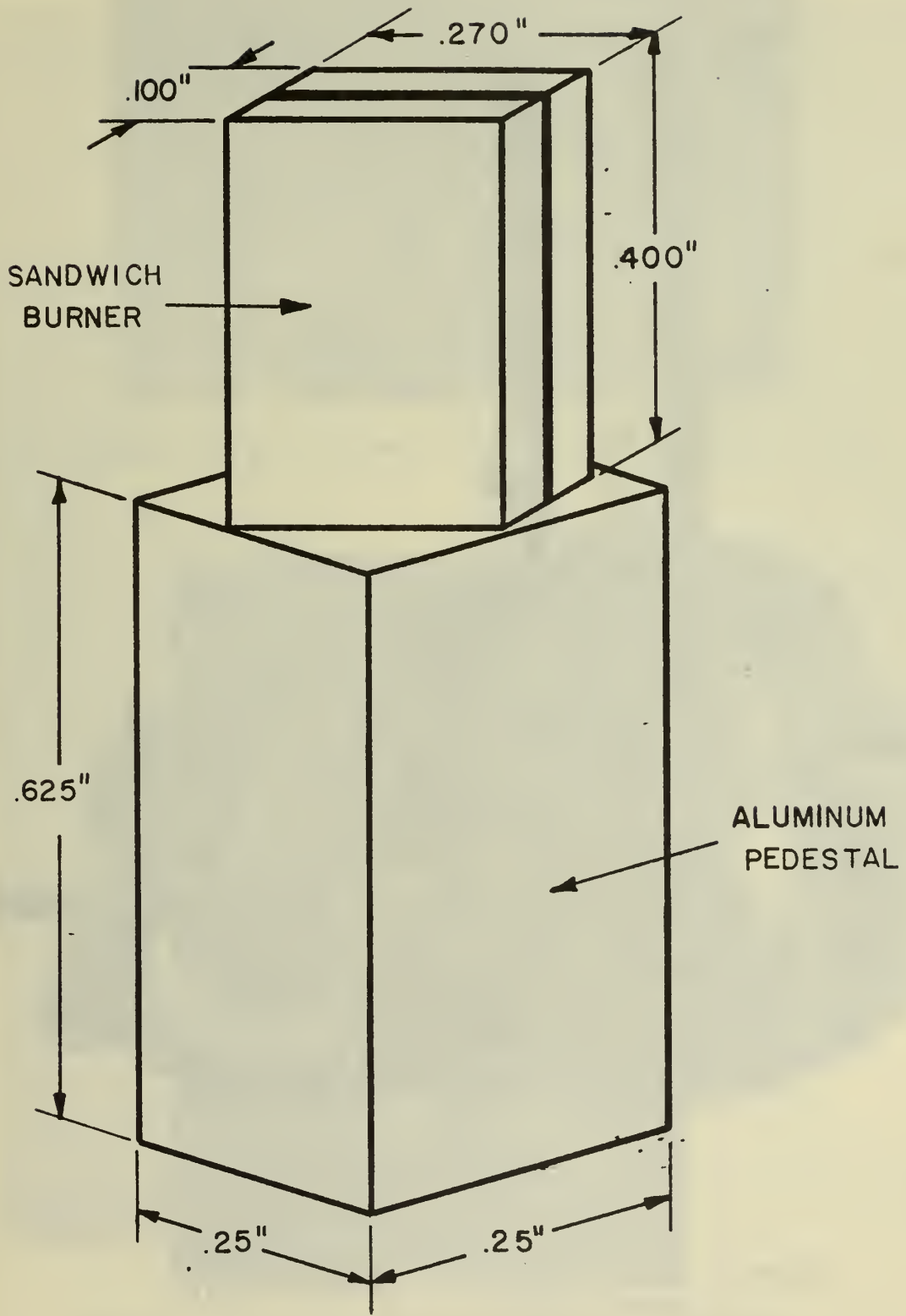


Figure 4 Schematic of Sandwich Burner



Figure 5 Combustion Bomb End Cap with Sandwich Burner Mounted

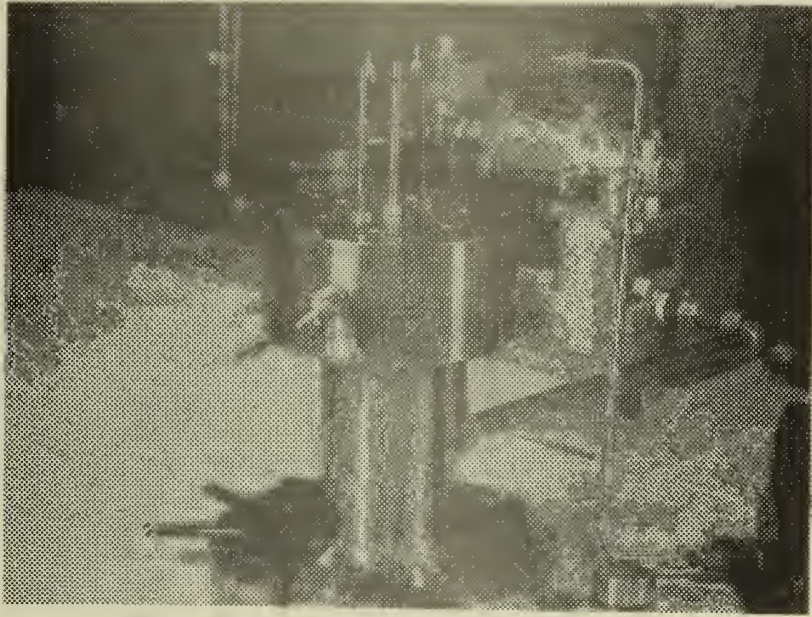


Figure 6 View of Assembled Base Section of Combustion Bomb



Figure 7 View of Assembled Combustion Bomb Along Optical Axis

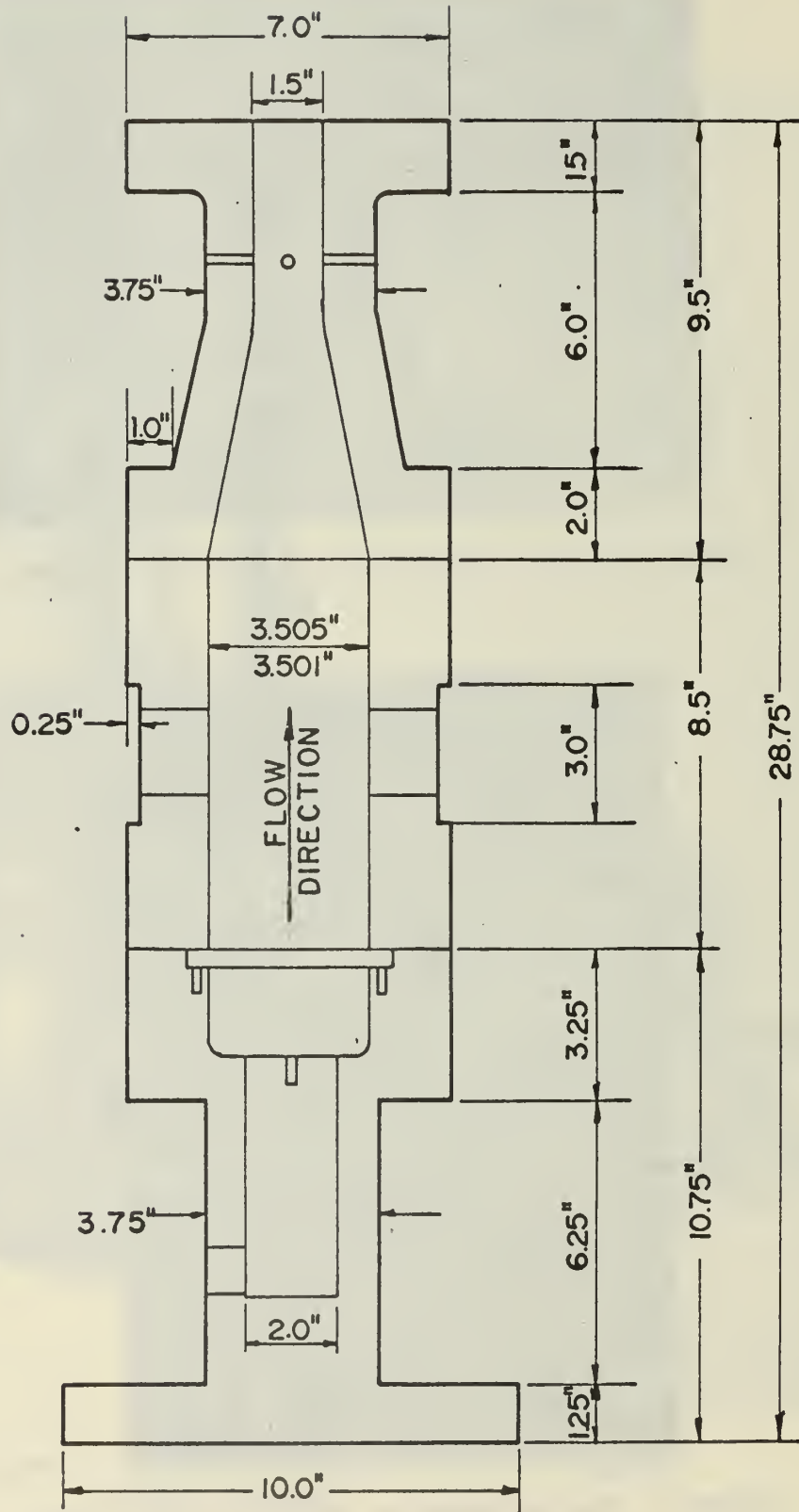


Figure 8 Schematic of Combustion Bomb

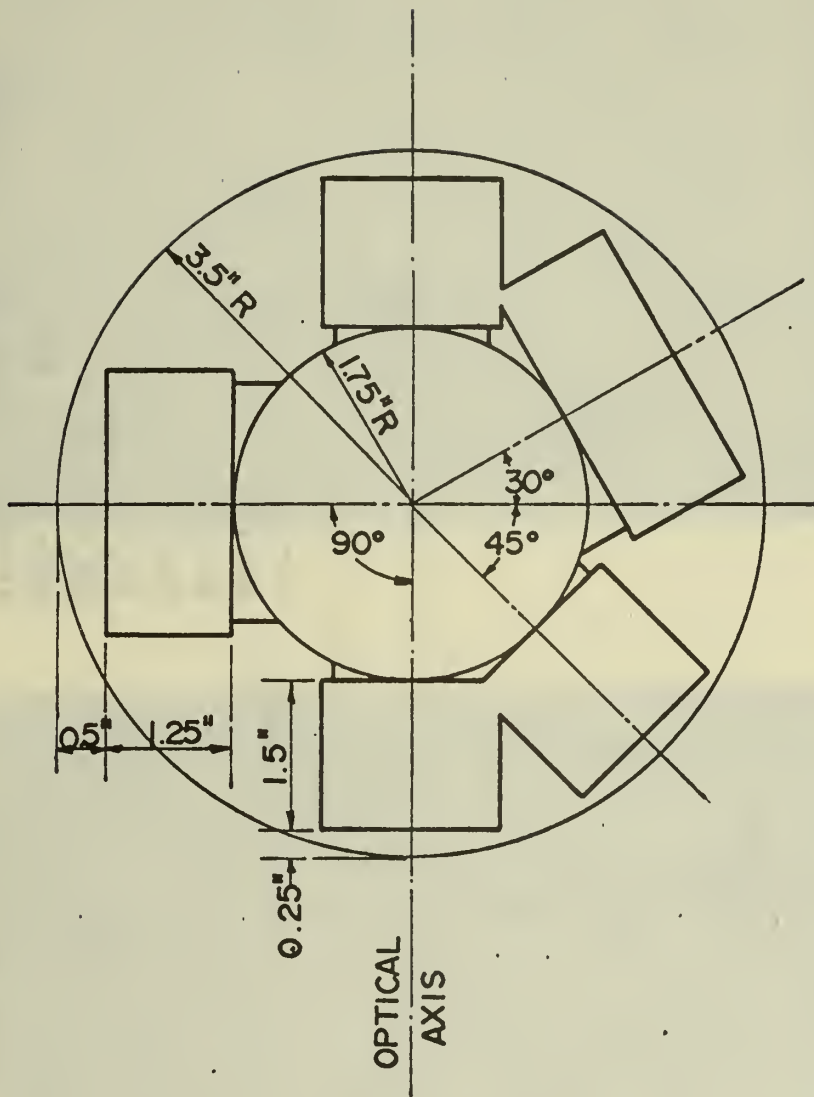


Figure 9 Angular Relationship of Bomb Windows

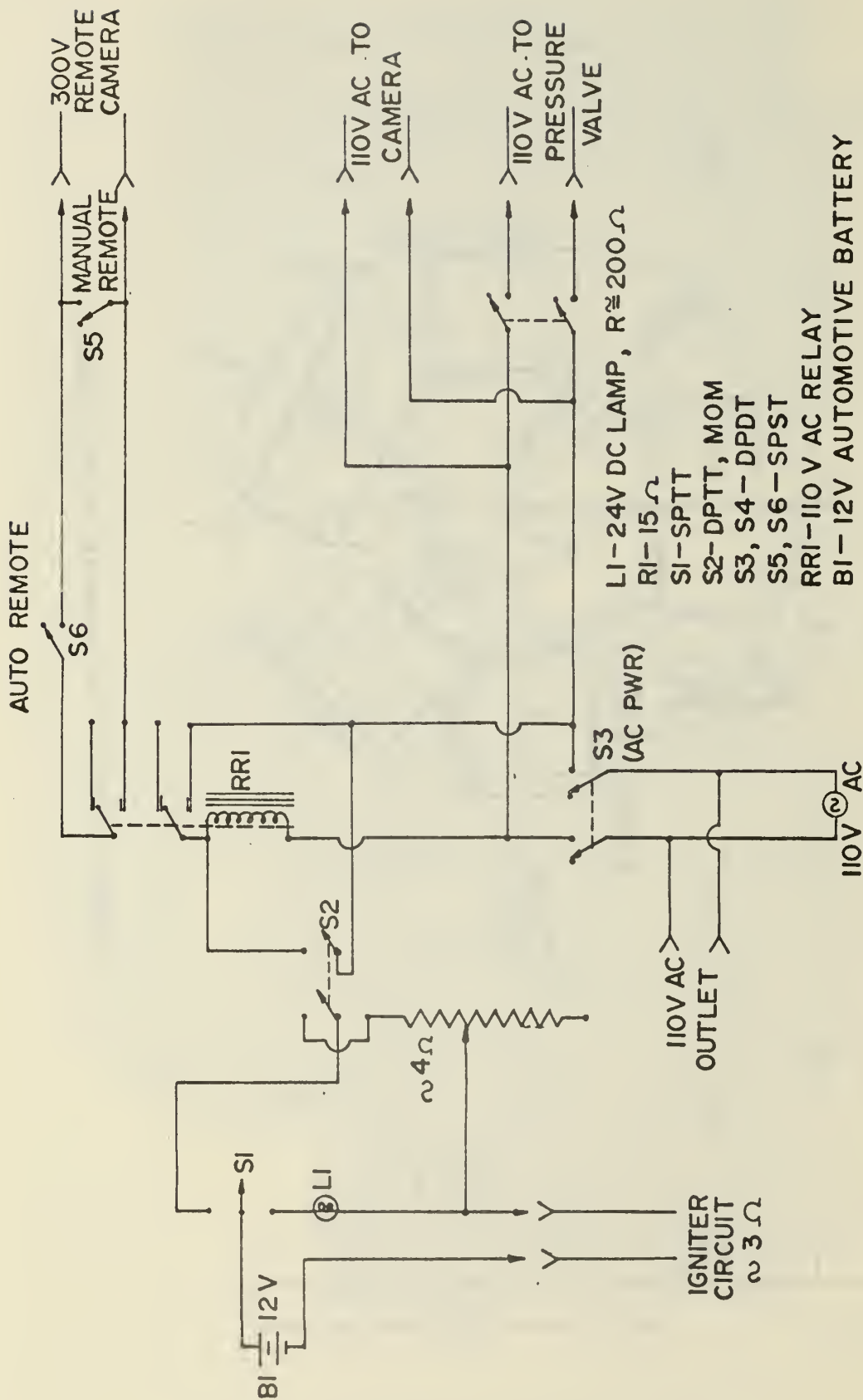
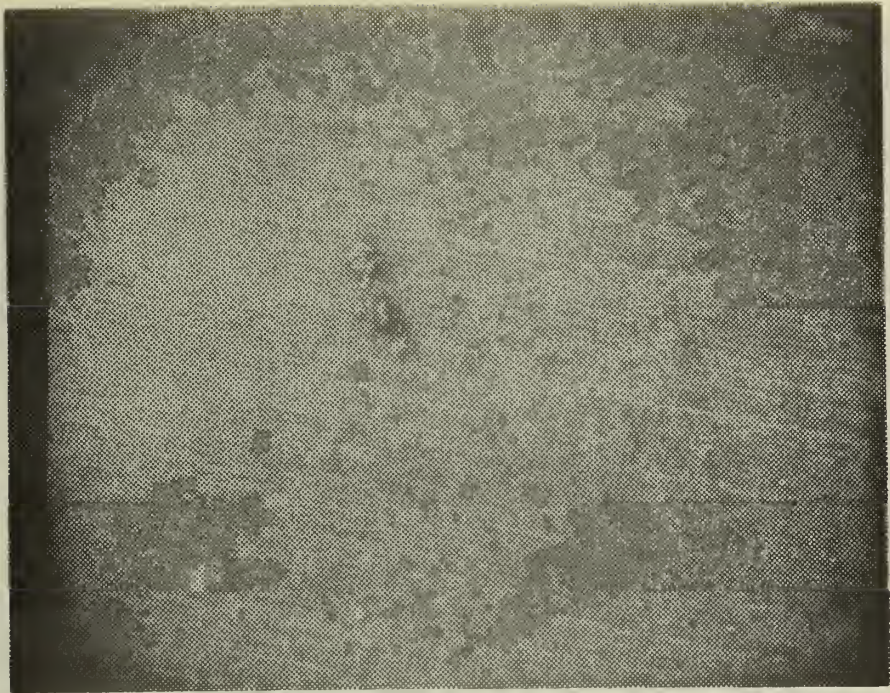
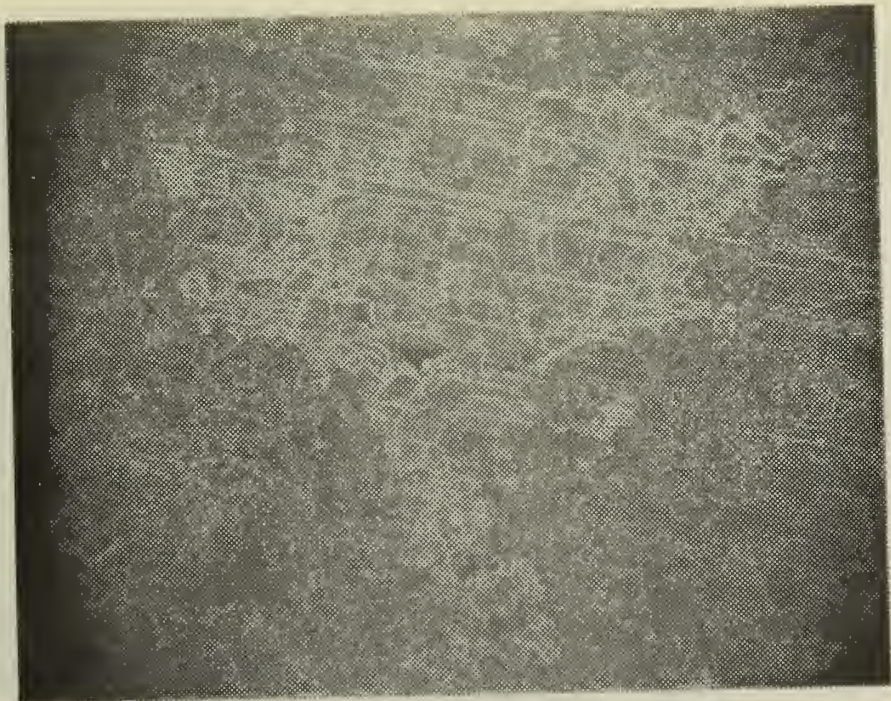


Figure 10 Electrical Schematic of Combustion Bomb Control Panel

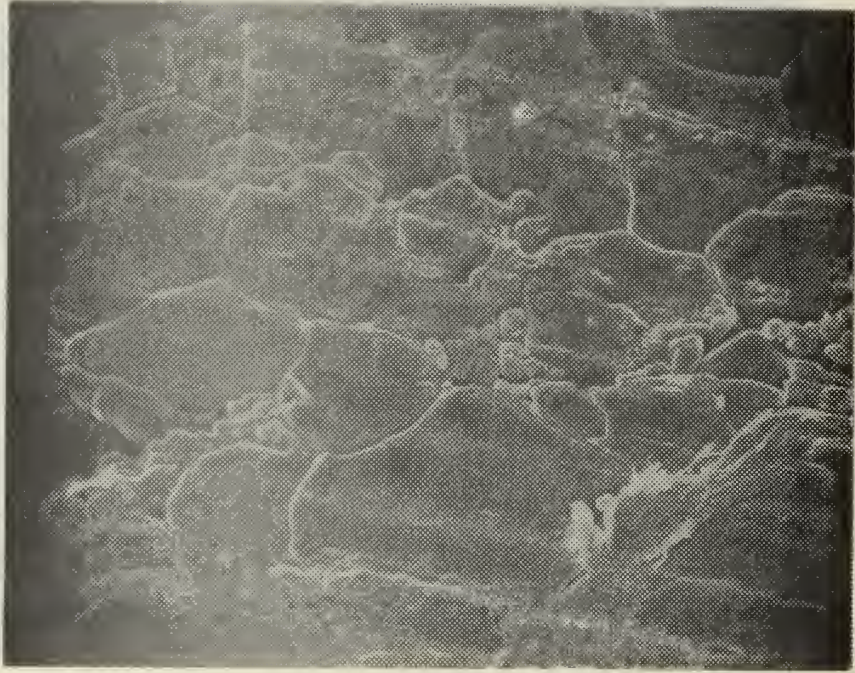


(a) 20X

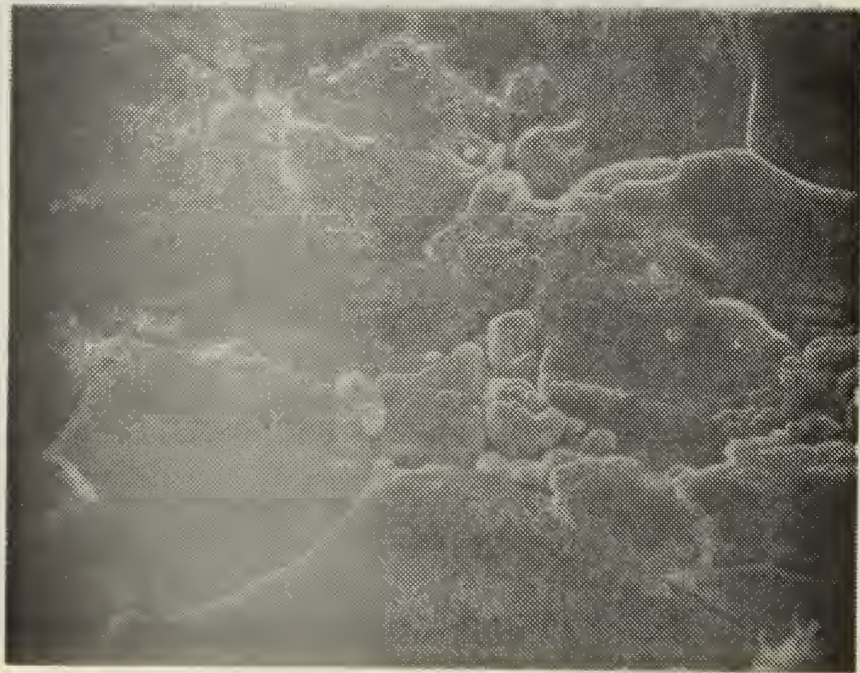


(b) 100X

Figure 11 Scanning Electron Microscope Photomicrographs
of High Purity AP Pellet Surface

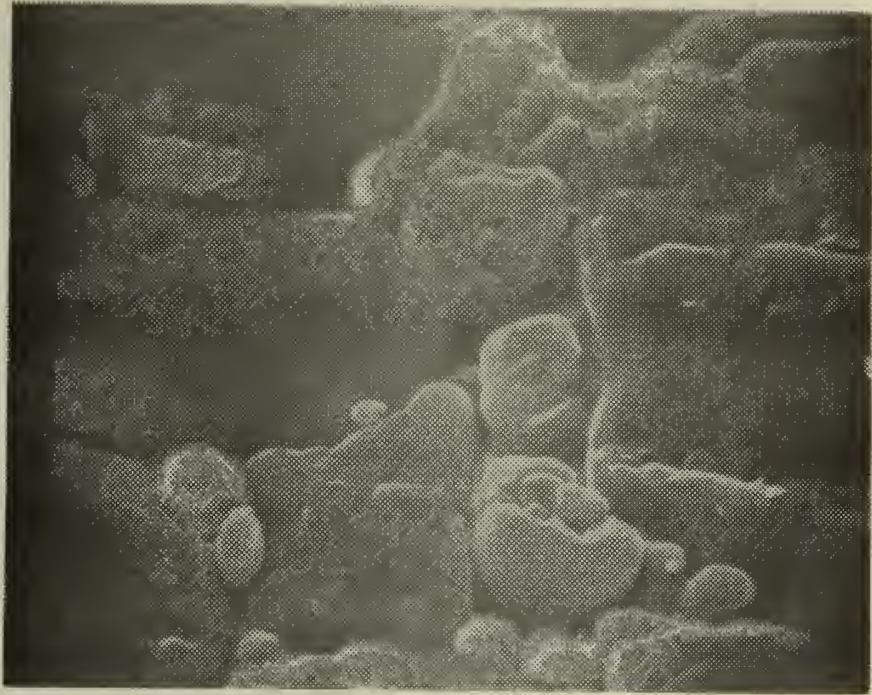


(c) 500X

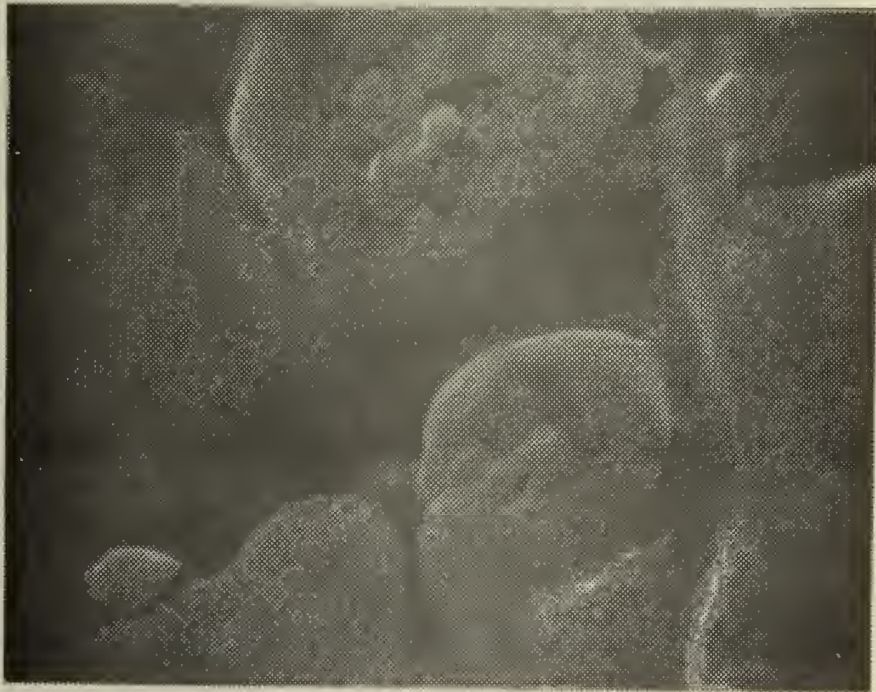


(d) 1000X

Figure 11 (Cont'd)

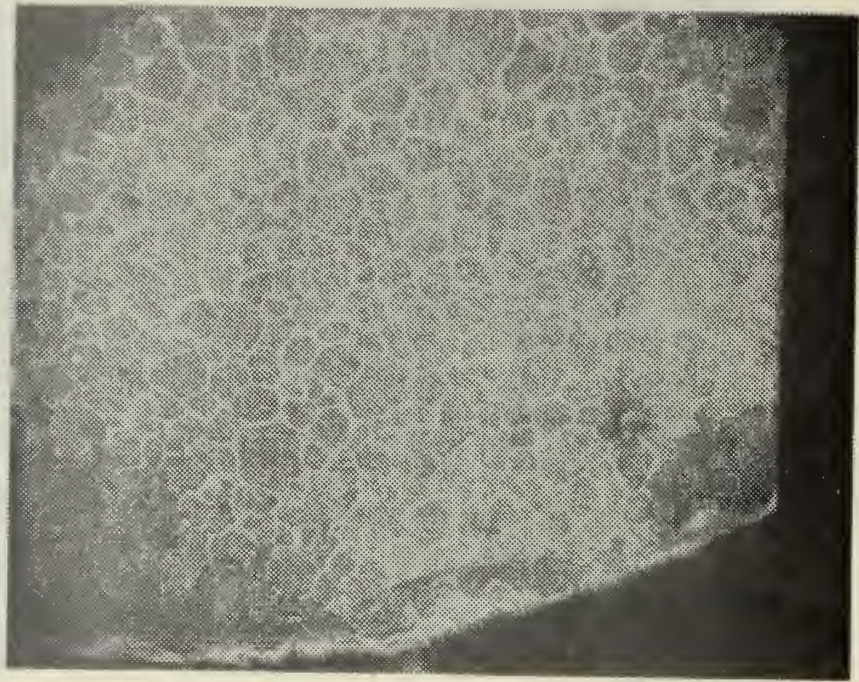


(e) 2000X

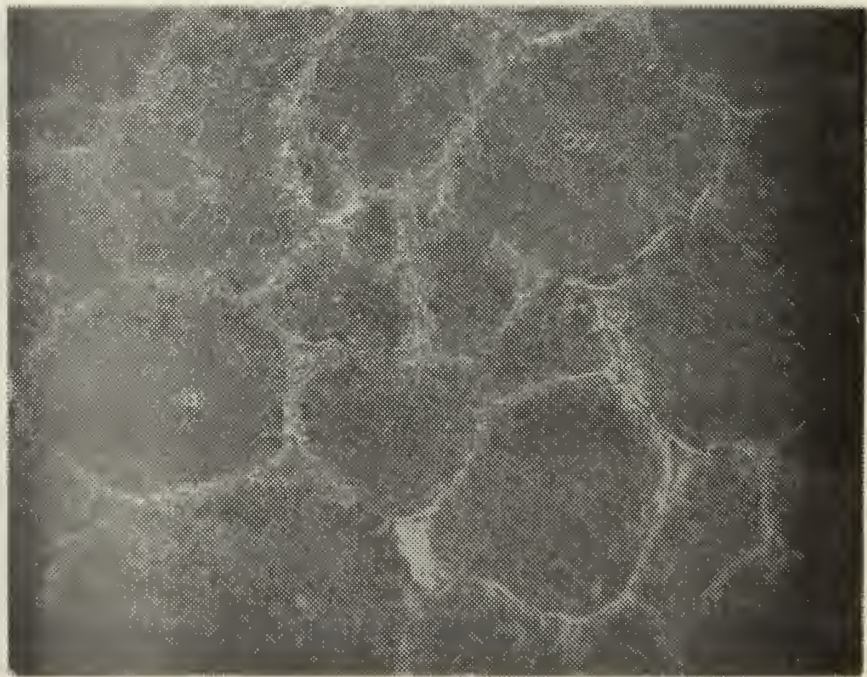


(f) 5000X

Figure 11 (Cont'd)

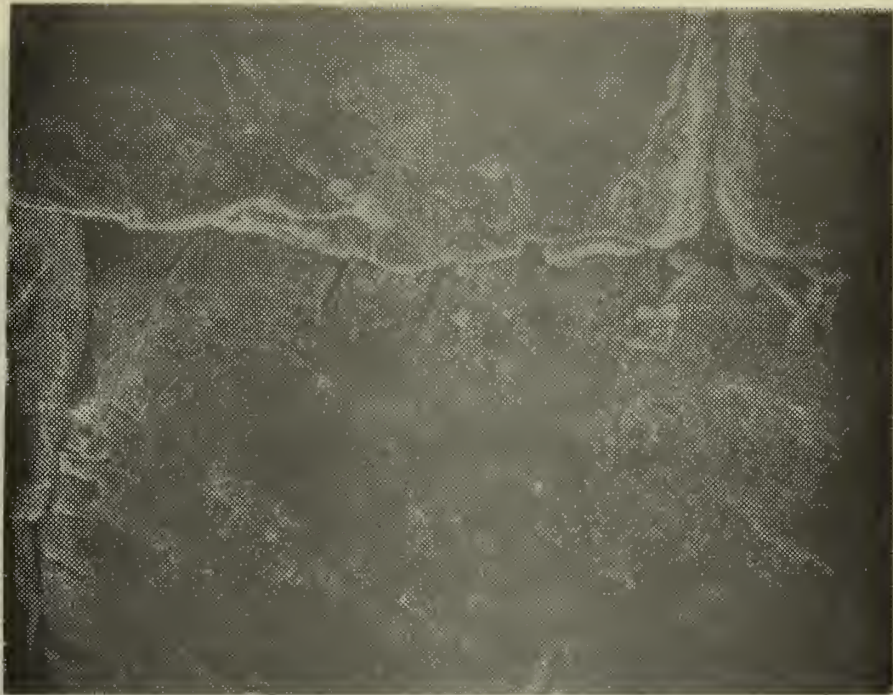


(a) 20X



(b) 100X

Figure 12 Scanning Electron Microscope Photomicrographs
of Propellant Grade AP (with TCP) Pellet Surface

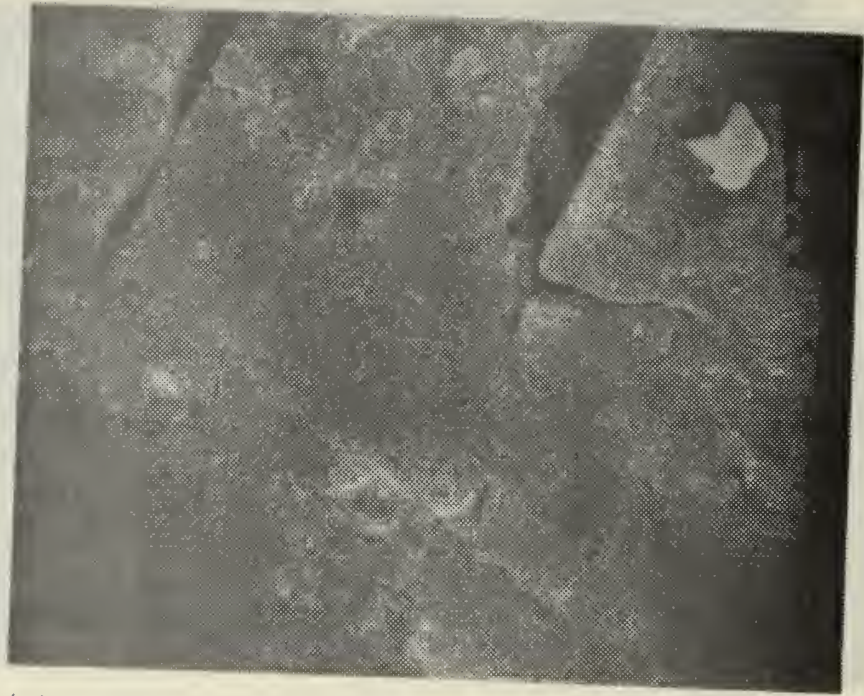


(c) 500X

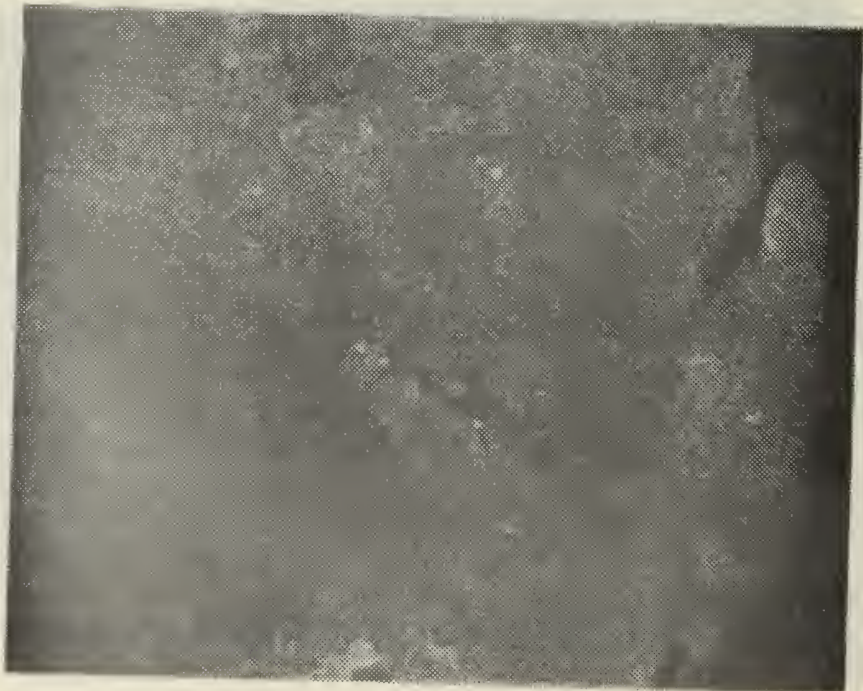


(d) 1000X

Figure 12 (Cont'd)

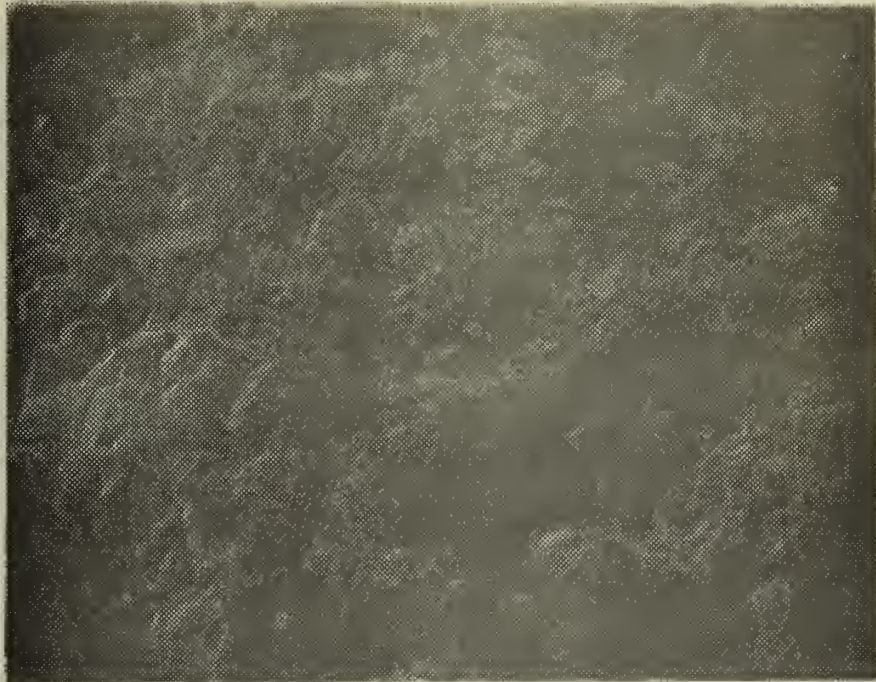


(e) 2000X

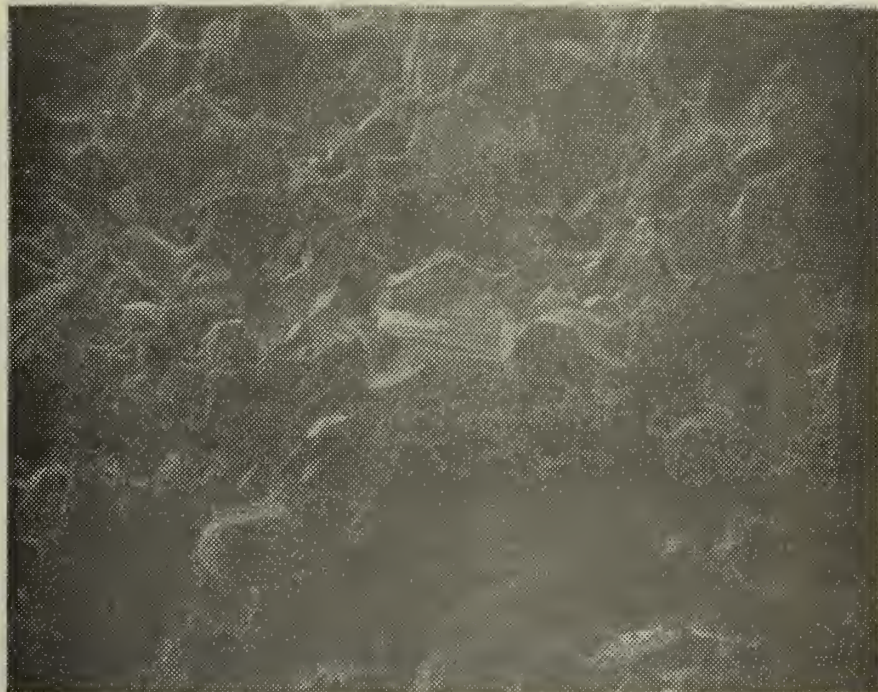


(f) 5000X

Figure 12 (Cont'd)

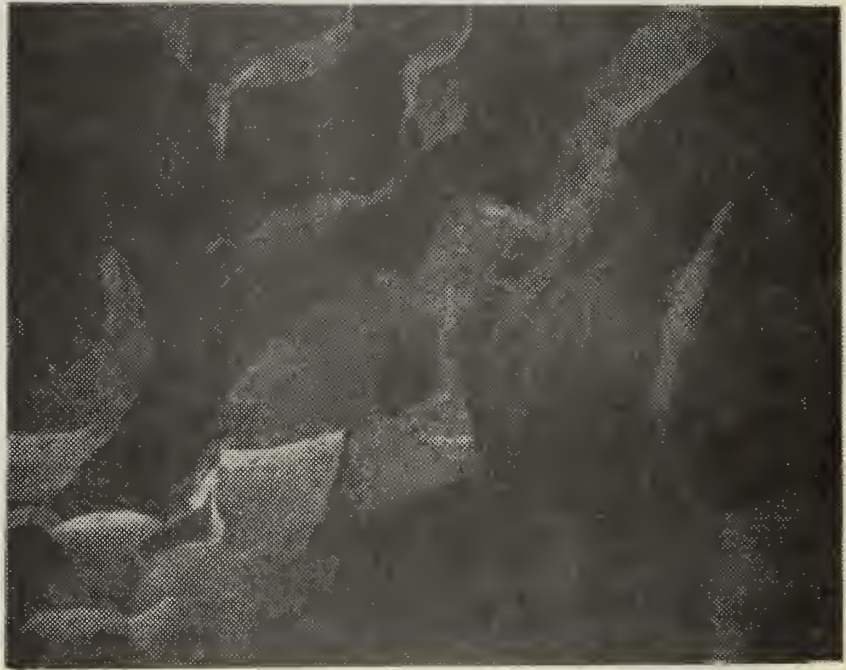


(a) 50X

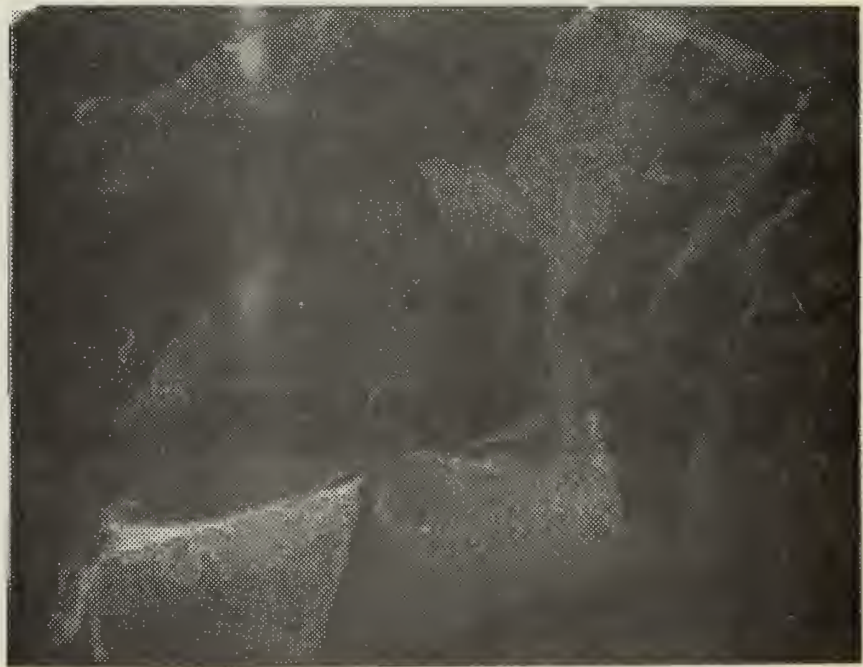


(b) 100X

Figure 13 Scanning Electron Microscope Photomicrographs
of High Purity AP Pellet Internal Structure



(c) 500X



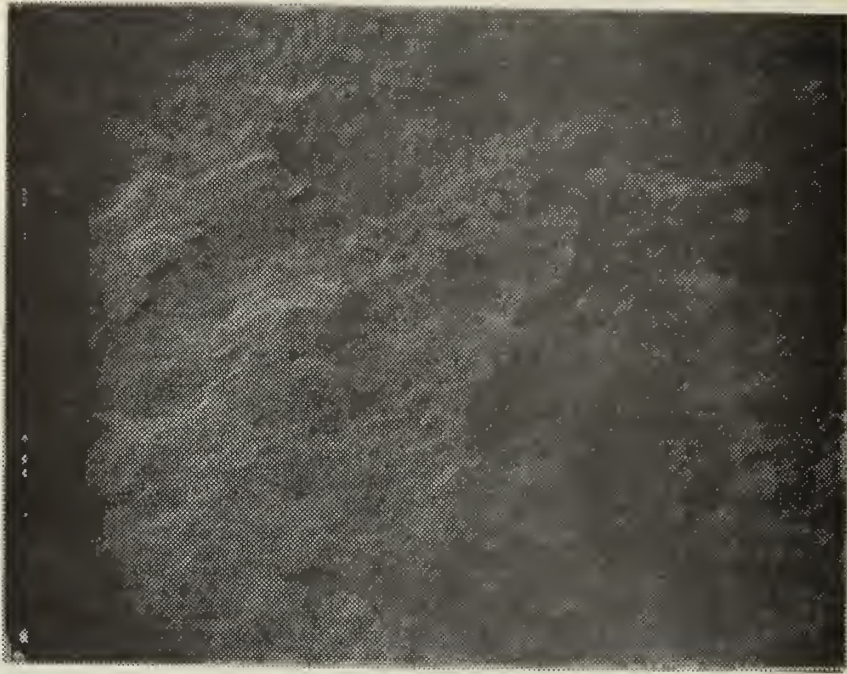
(d) 1000X

Figure 13 (Cont'd)

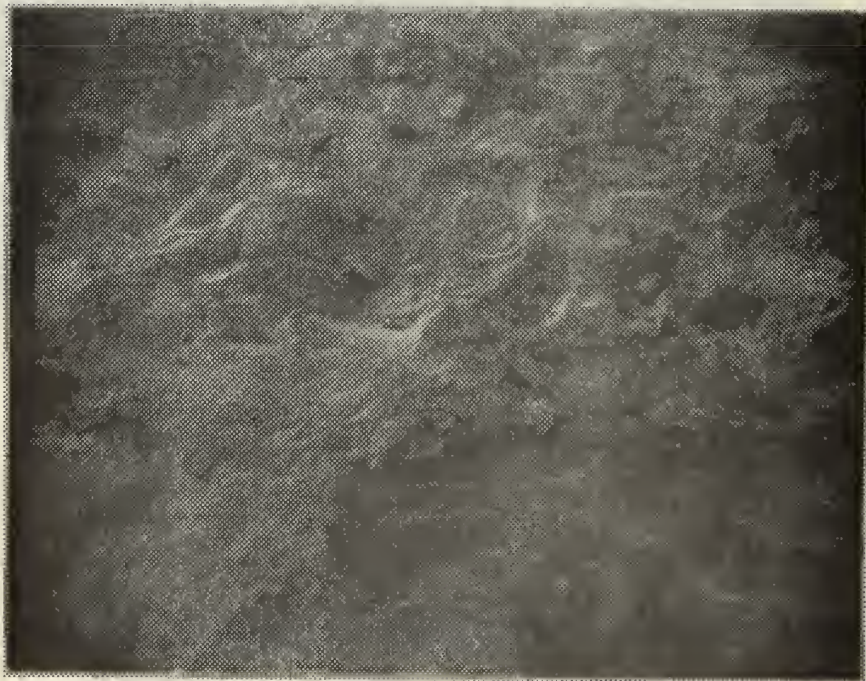


(e) 2000X

Figure 13 (Cont'd)

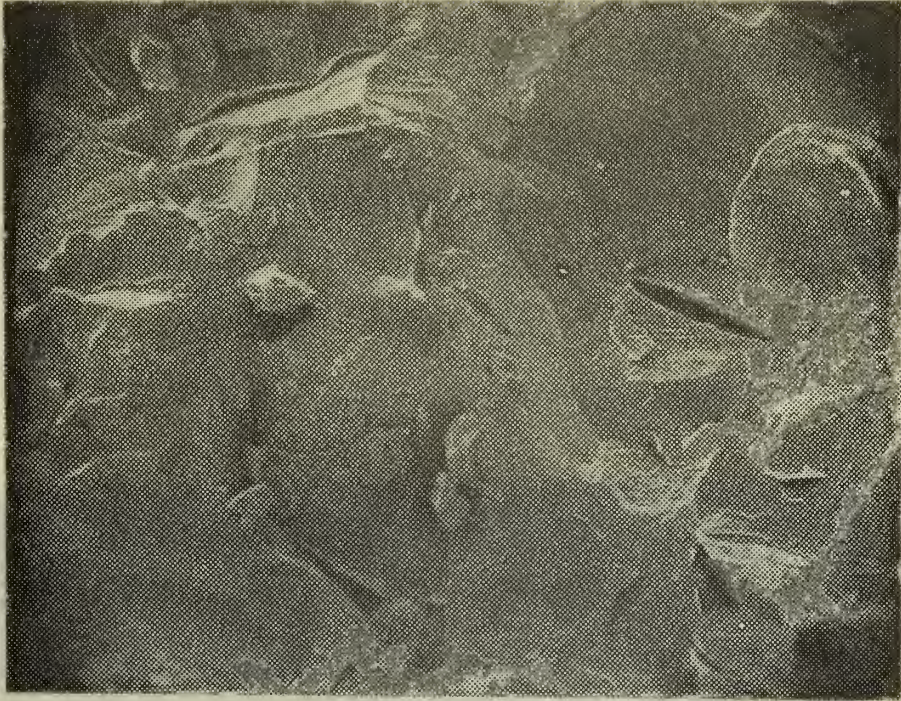


(a) 50X

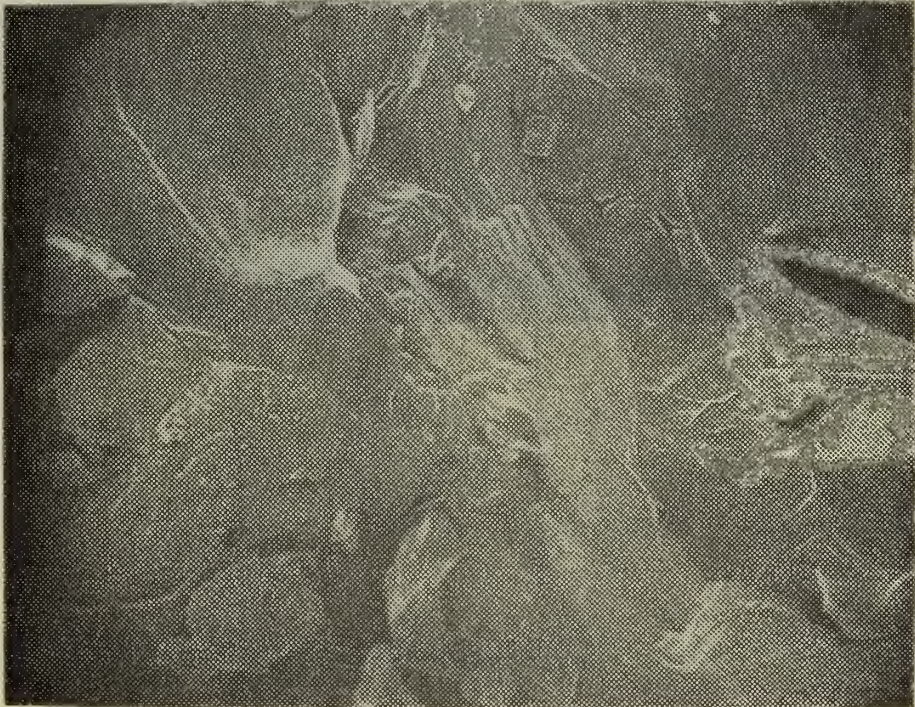


(b) 100X

Figure 14 Scanning Electron Microscope Photomicrographs of Propellant Grade AP (with TCP) Pellet Internal Structure

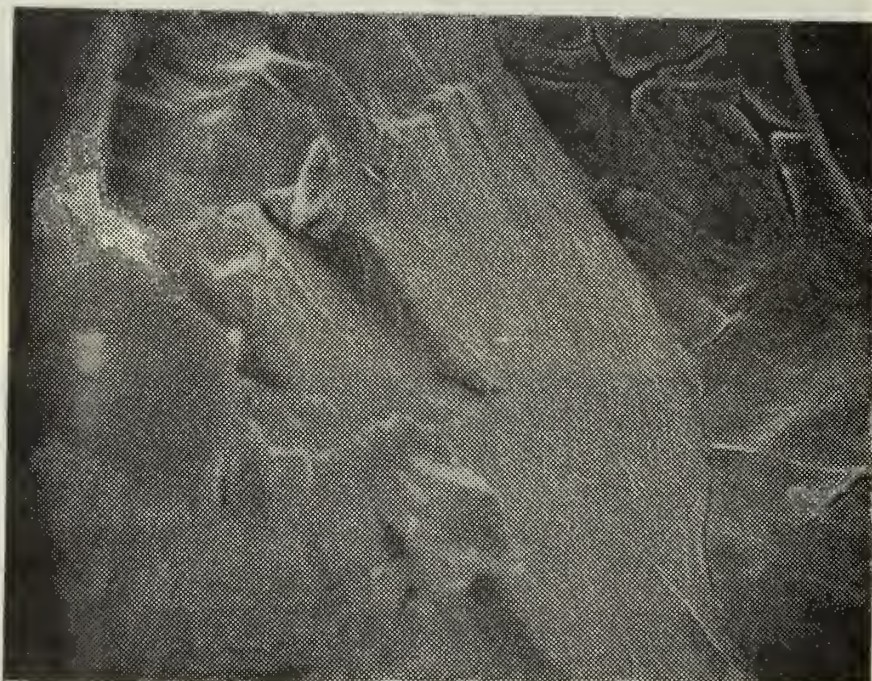


(c) 500X



(d) 1000X

Figure 14 (Cont'd)



(e) 2000X

Figure 14 (Cont'd)

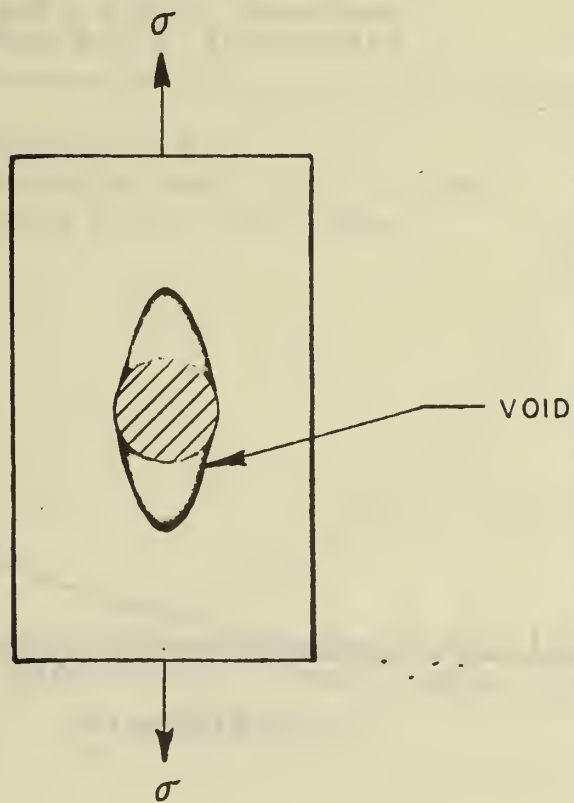
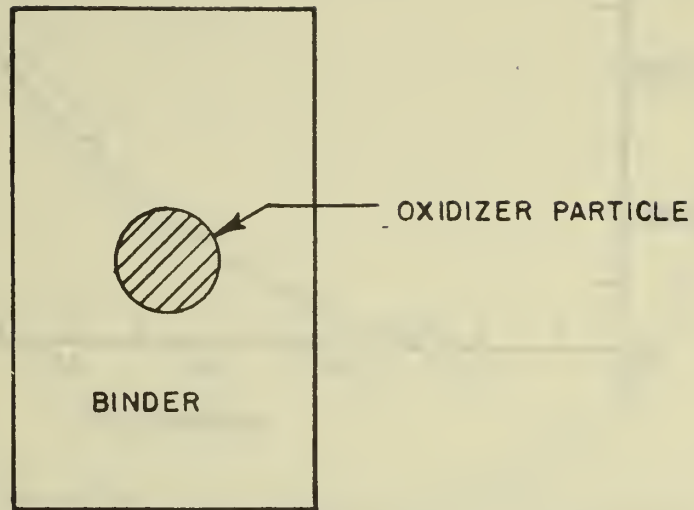


Figure 15 Void Formation Upon Dewetting

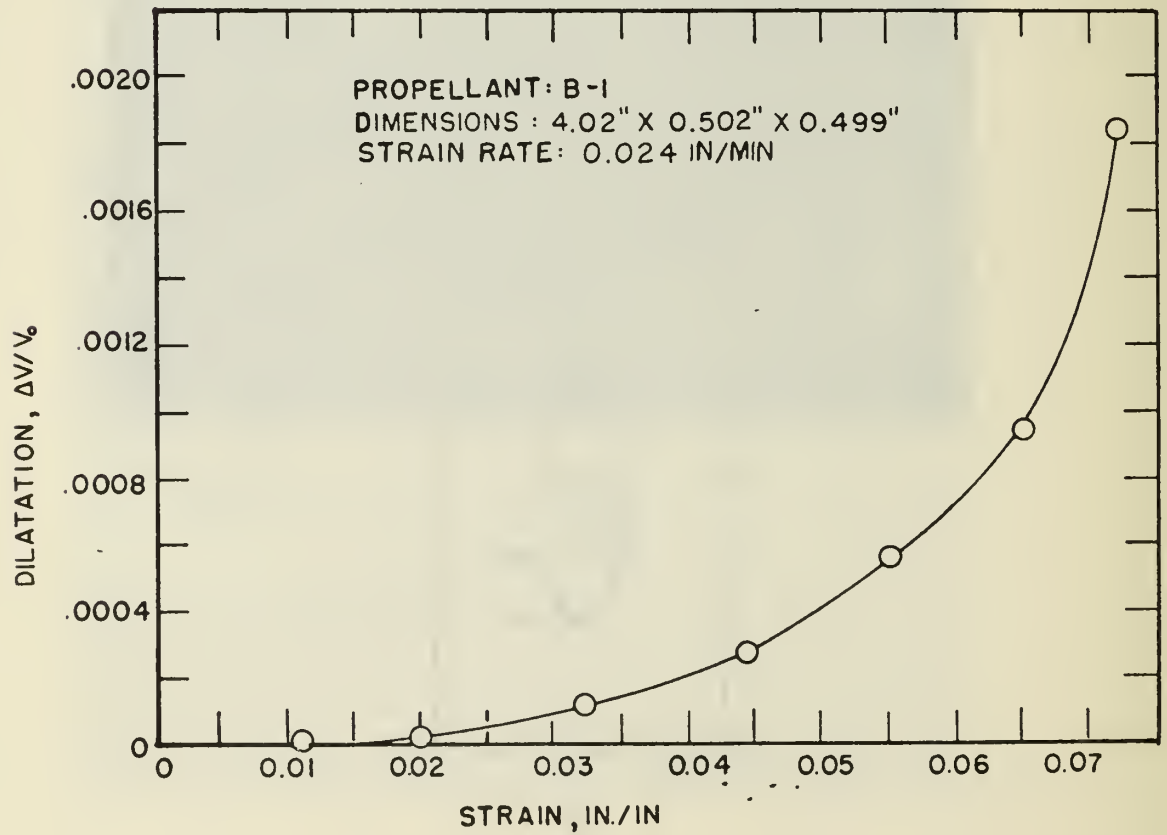
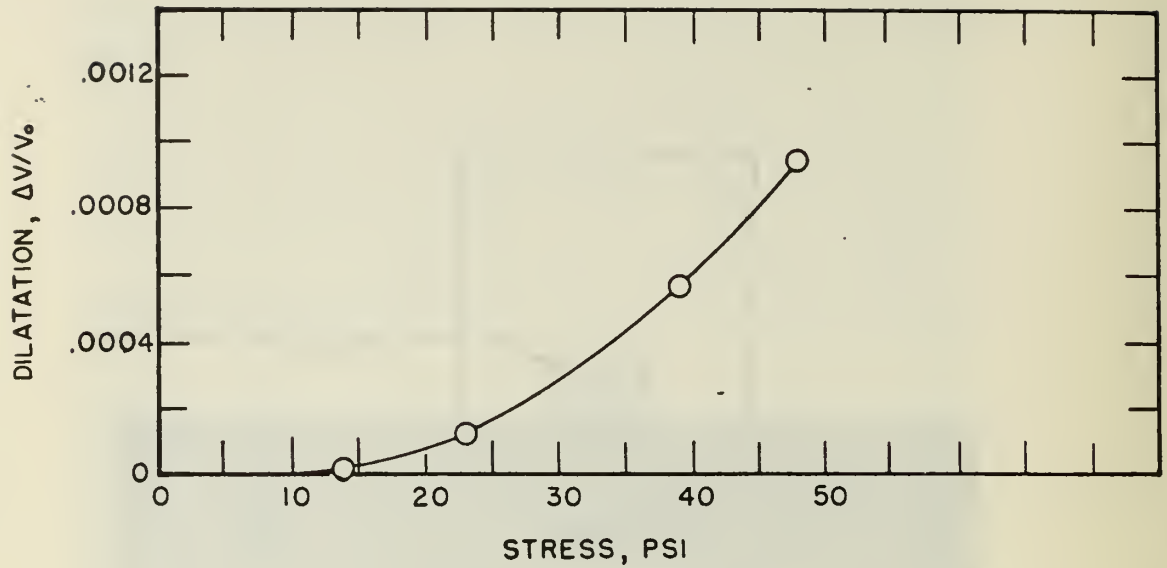


Figure 16 Dilatation vs Stress and Strain for Propellant B-1

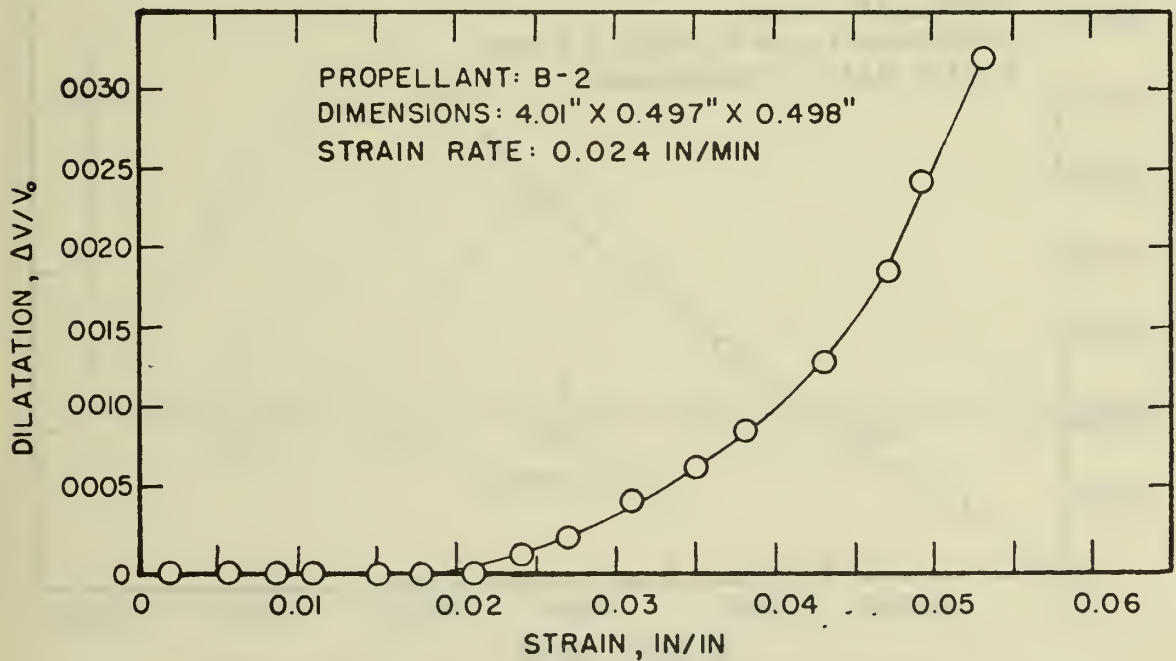
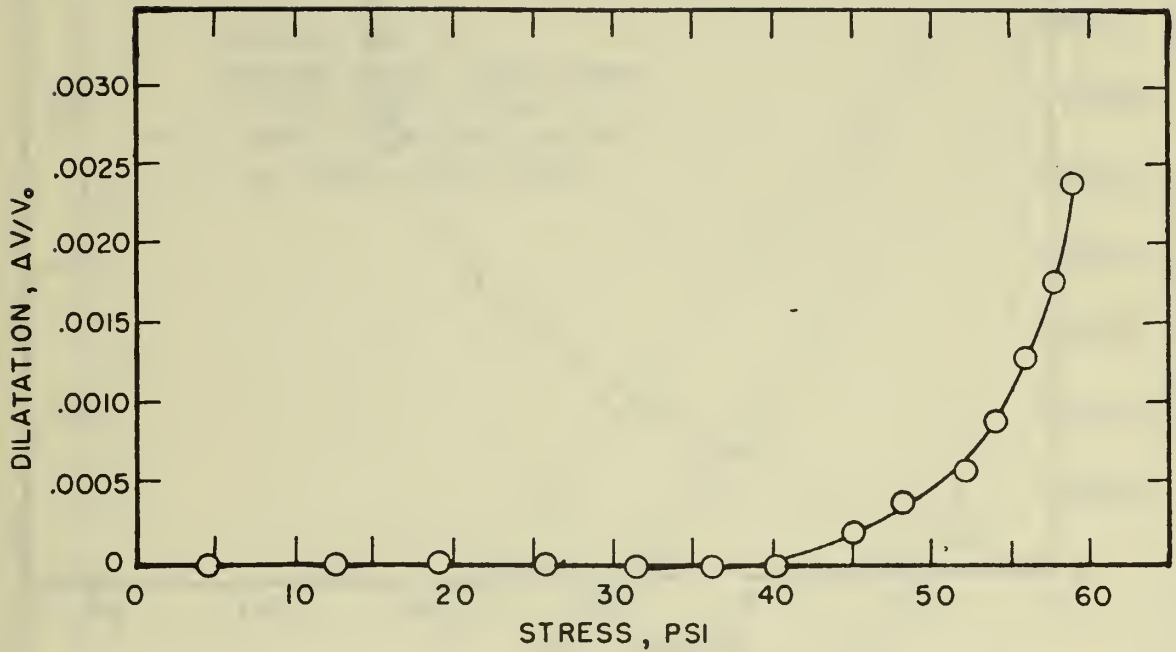


Figure 17 Dilatation vs Stress and Strain for Propellant B-2

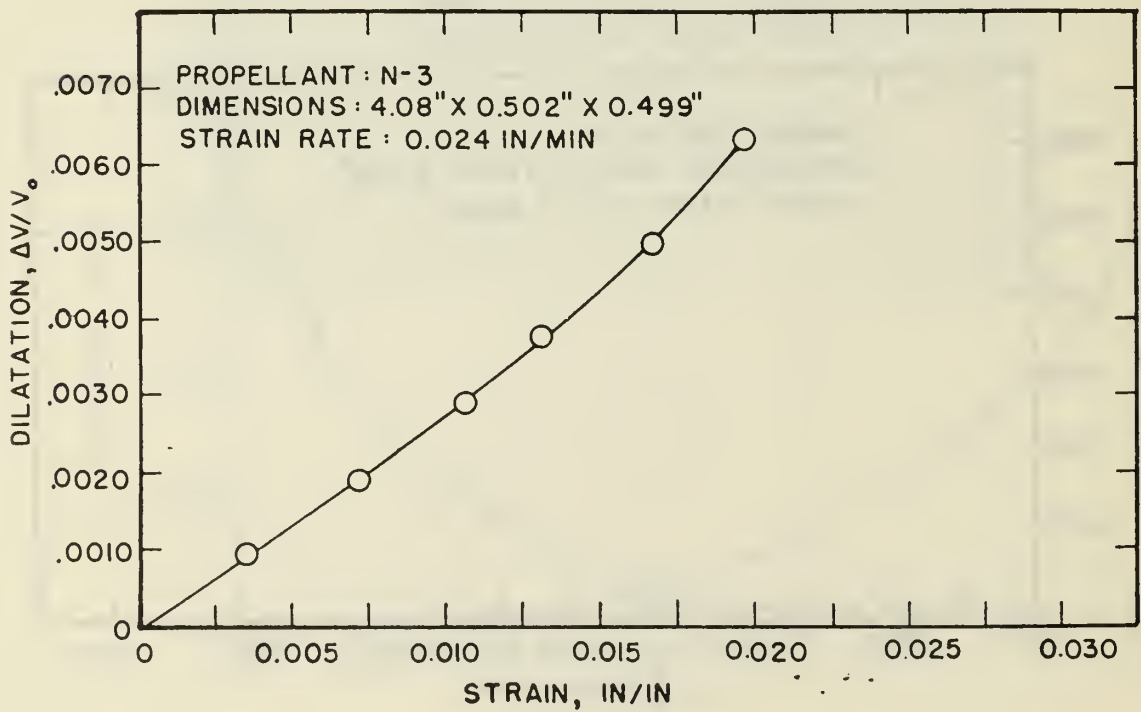
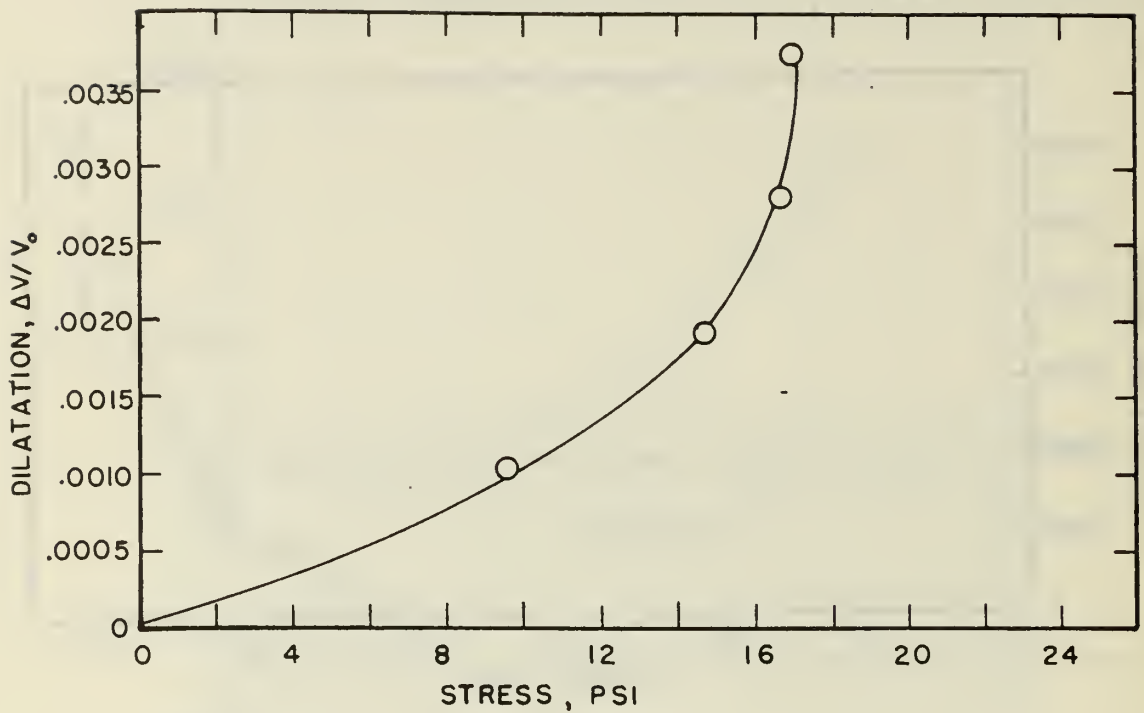


Figure 18 Dilatation vs Stress and Strain for Propellant N-3

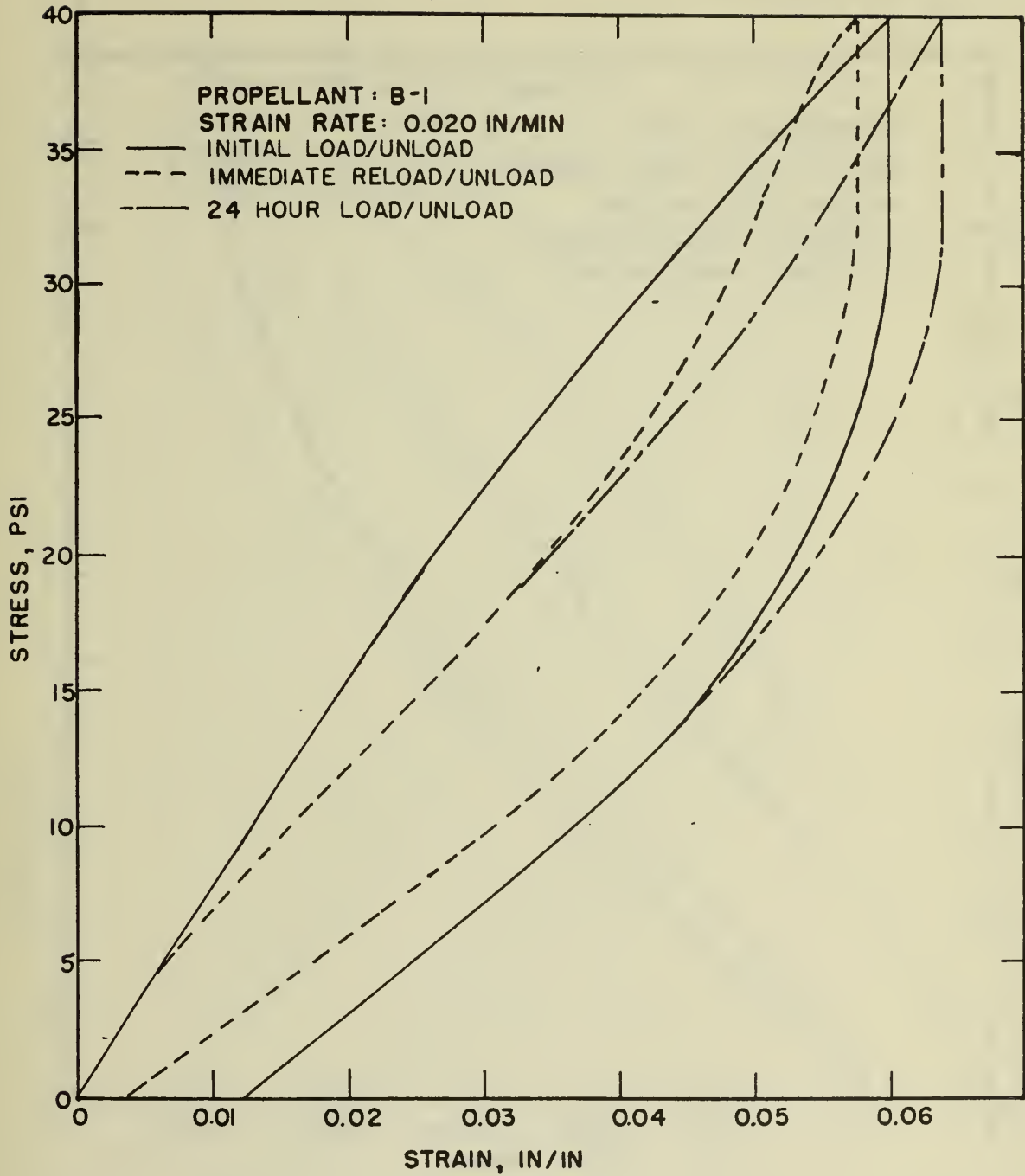


Figure 19 Stress vs Strain for Propellant B-1

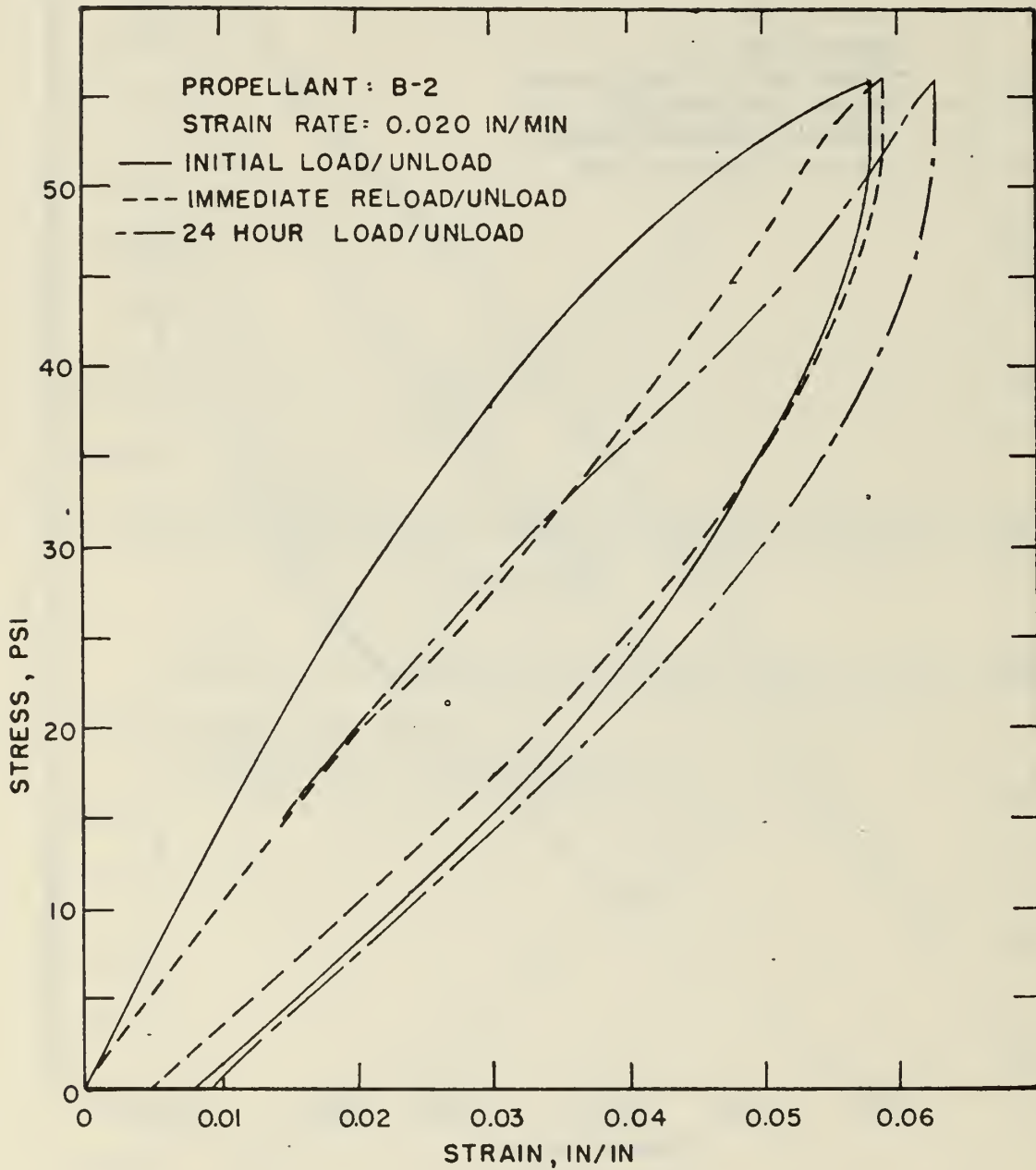


Figure 20 Stress vs Strain for Propellant B-2

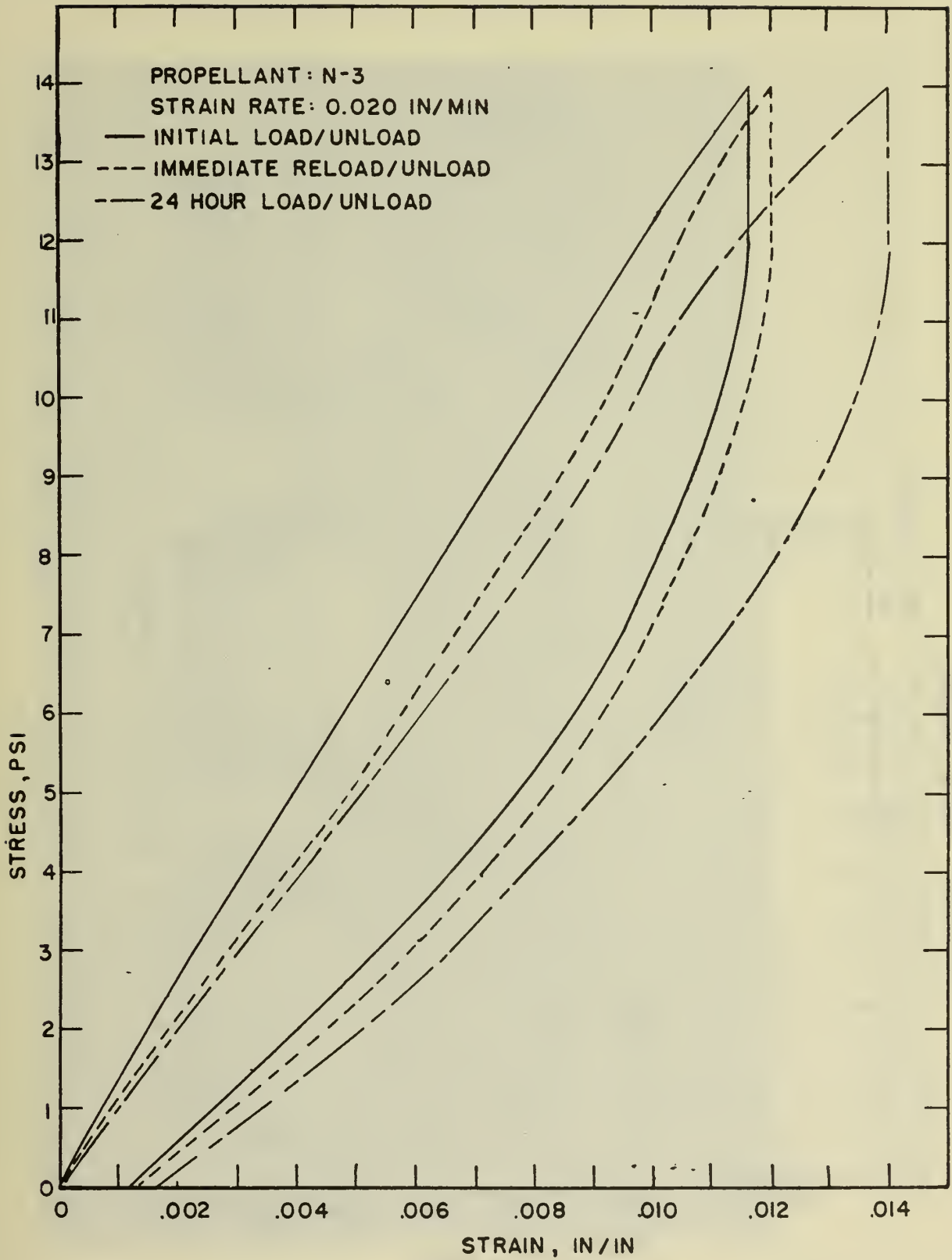


Figure 21 Stress vs Strain for Propellant N-3

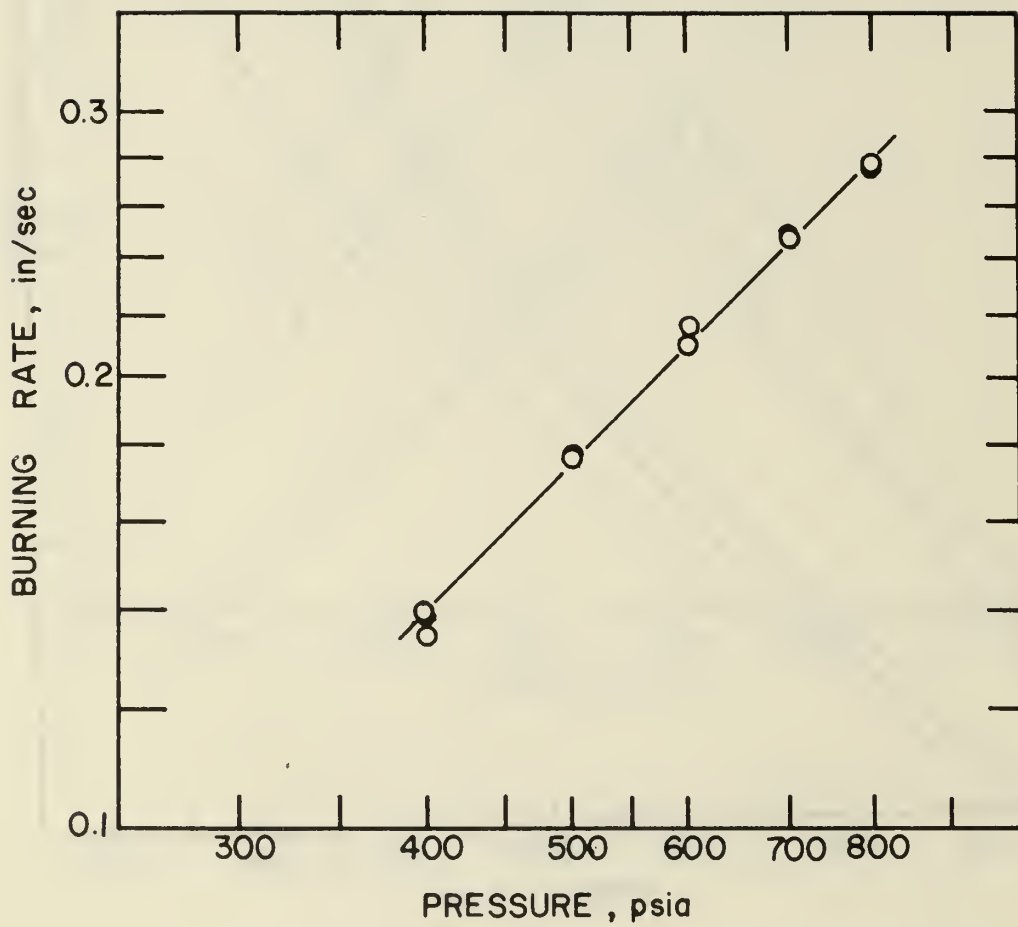


Figure 22 AP Pellet Burning Rate vs Pressure

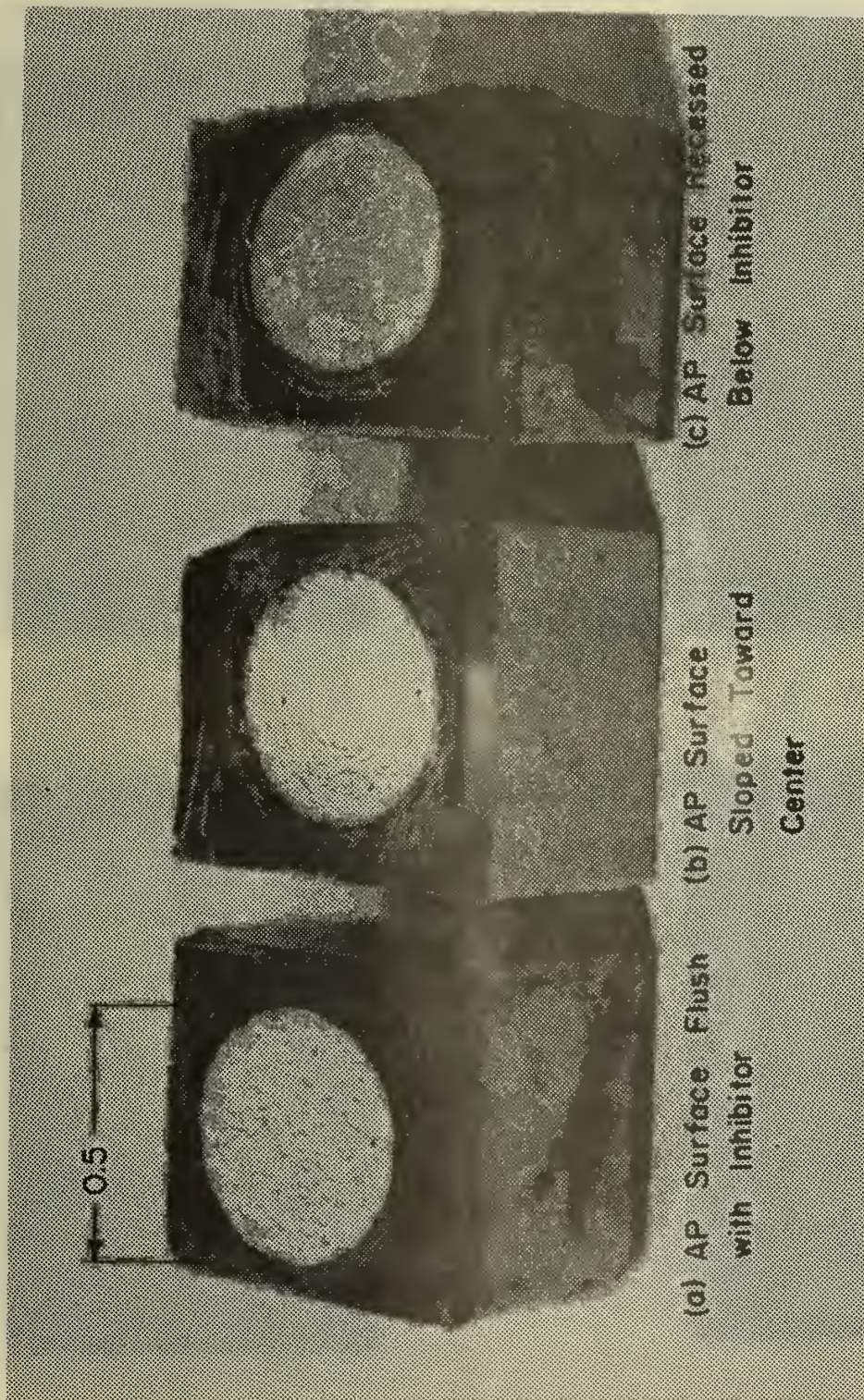


Figure 23 Photograph of Self Extinguished AP Pellets



(a) 200 psi, 0g



(b) 200 psi, 100g



(c) 500 psi, 0g



(d) 500 psi, 100g

Figure 24 Burn Profiles of AP(UHP)/PBAA Sandwich Tests



(e) 800 psi, 0g



(f) 800 psi, 100g

Figure 24 (Cont'd)



(a) 200 psi, 0g



(b) 200 psi, 100g



(c) 500 psi, 0g



(d) 500 psi, 100g

Figure 25 Burn Profiles of AP (TCP/PBAA Sandwich Tests



(e) 800 psi, 0g

Figure 25 (Cont'd)



Figure 26 Color Photograph of PBAA/AP Sandwich
Burning at 800 psi

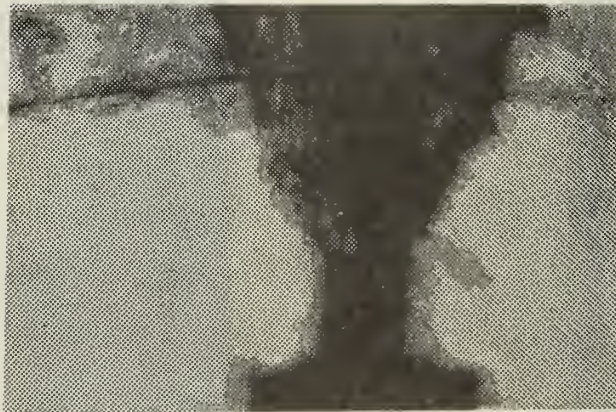


Figure 27 Color Schlieren of PBAA/AP Sandwich
Burning at 800 psi

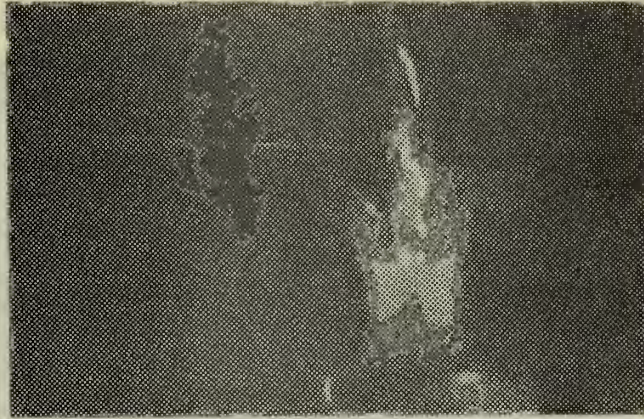


Figure 28 Color Photograph of PBAA/AP Sandwich
Burning at 500 psi

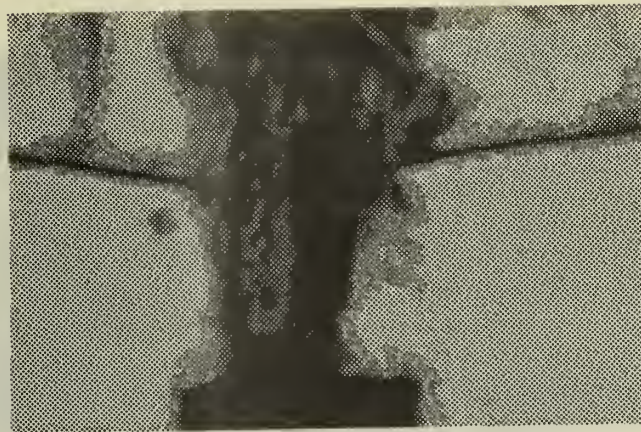


Figure 29 Color Schlieren of PBAA/AP Sandwich
Burning at 500 psi



Figure 30 Color Photograph of PBAA/AP Sandwich Burning at 200 psi



Figure 31 Color Schlieren of PBAA/AP Sandwich Burning at 200 psi

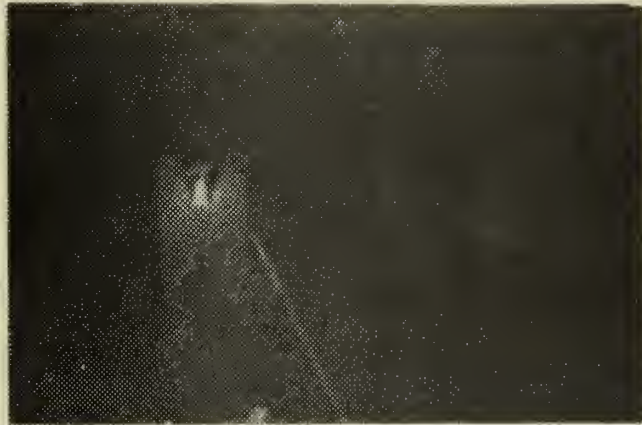


Figure 32 Color Photograph of PBAA/AP Sandwich
Burning at 100 psi

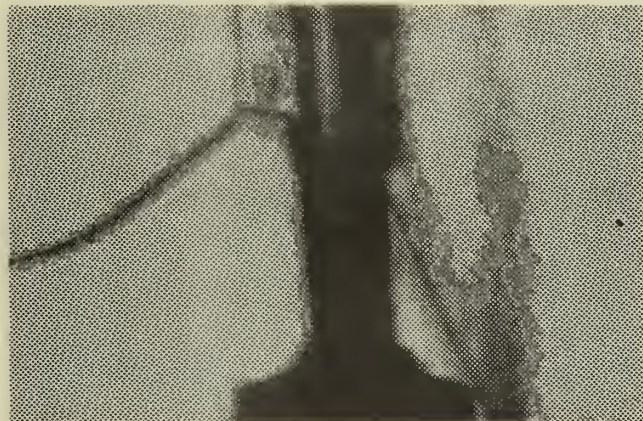


Figure 33 Color Schlieren of PBAA/AP Sandwich
Burning at 100 psi



Figure 34 Color Schlieren of PBAA/AP Sandwich
Burning at 100 psi, Horizontal Color Matrix



Figure 35 Color Photograph of PBAA/AP Sandwich
Burning at 500 psi, Side View

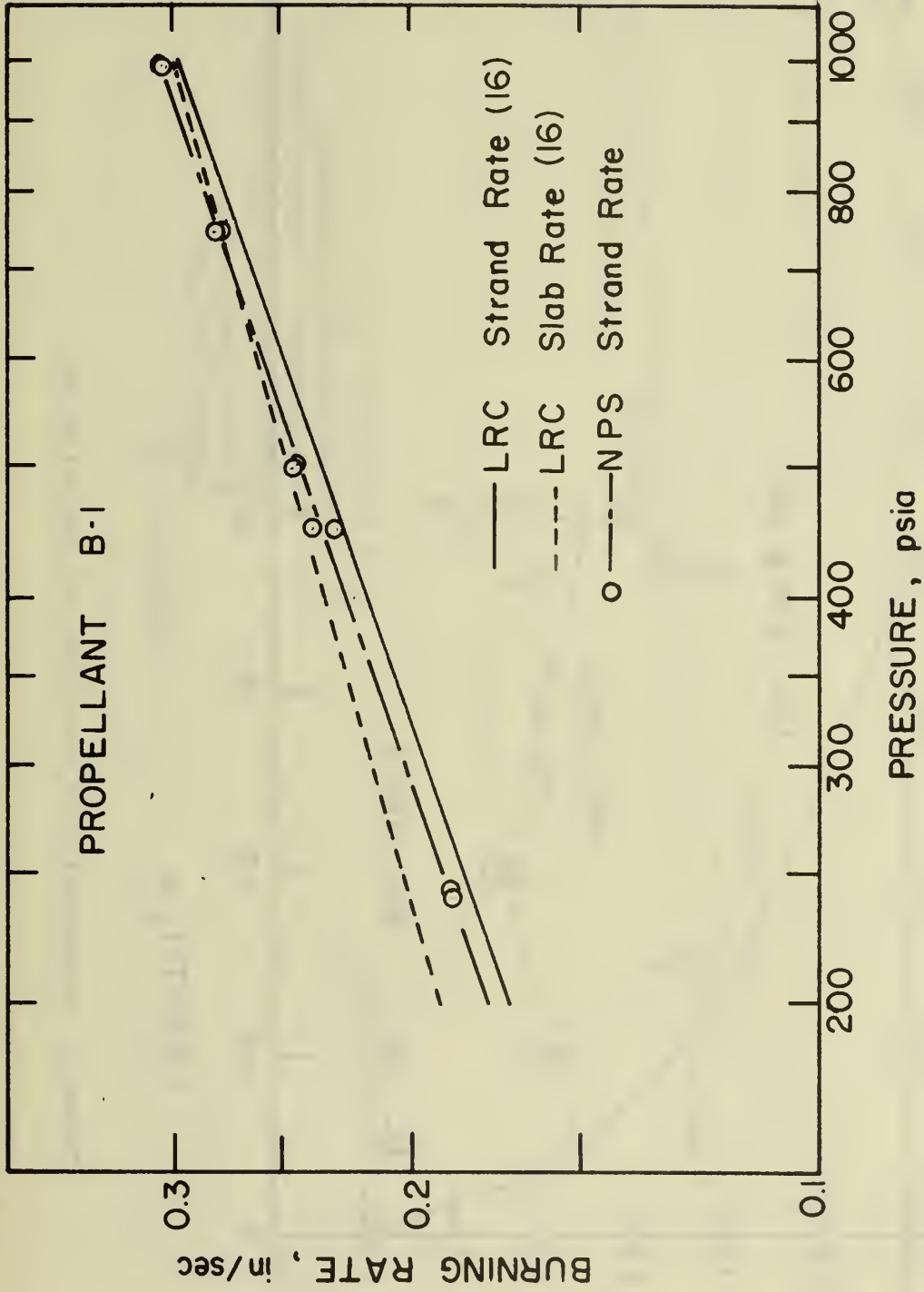


Figure 36 Burning Rate vs Pressure for Propellant B-1

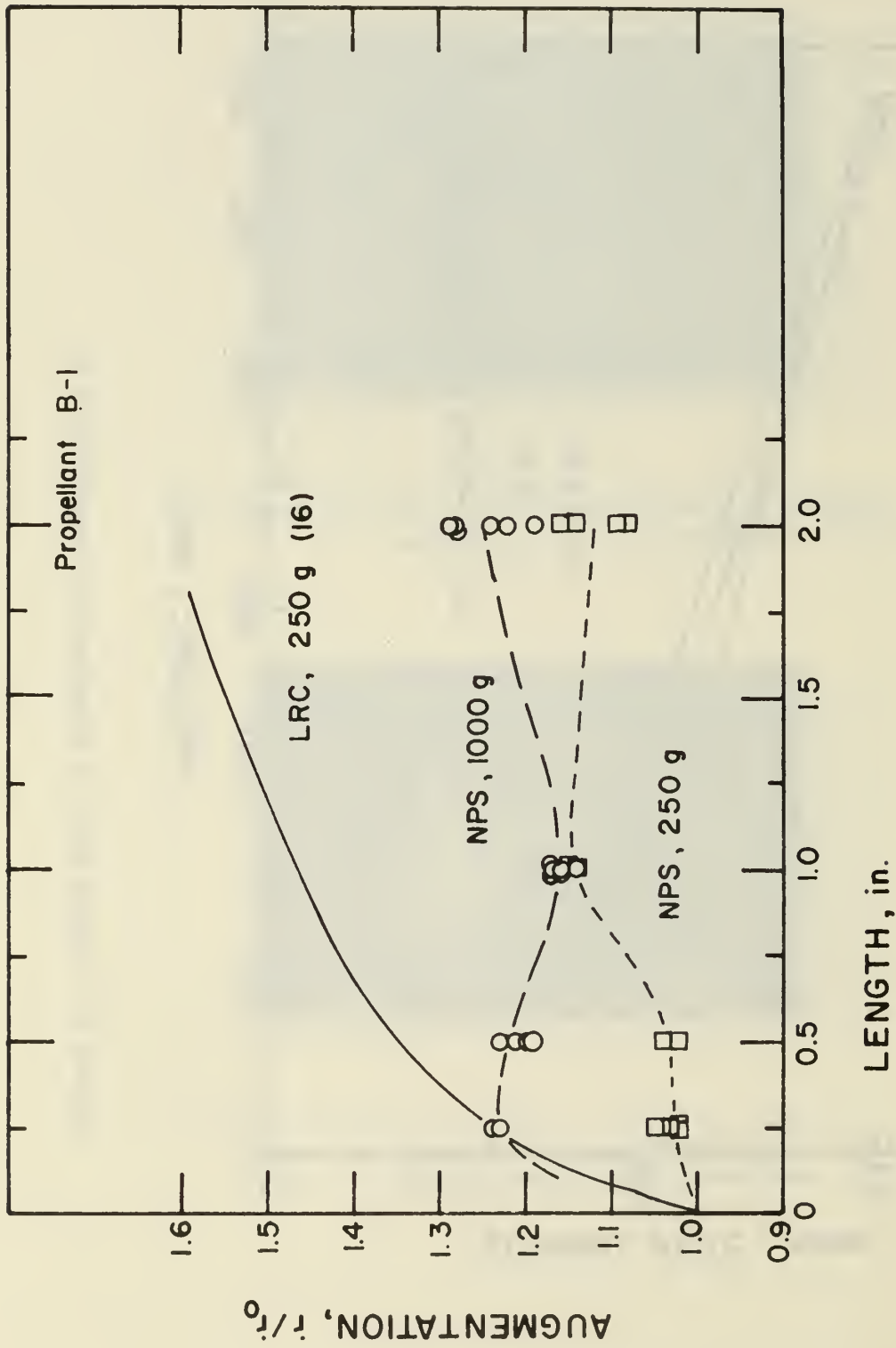


Figure 37 Augmentation vs Burn Time for Propellant B-1

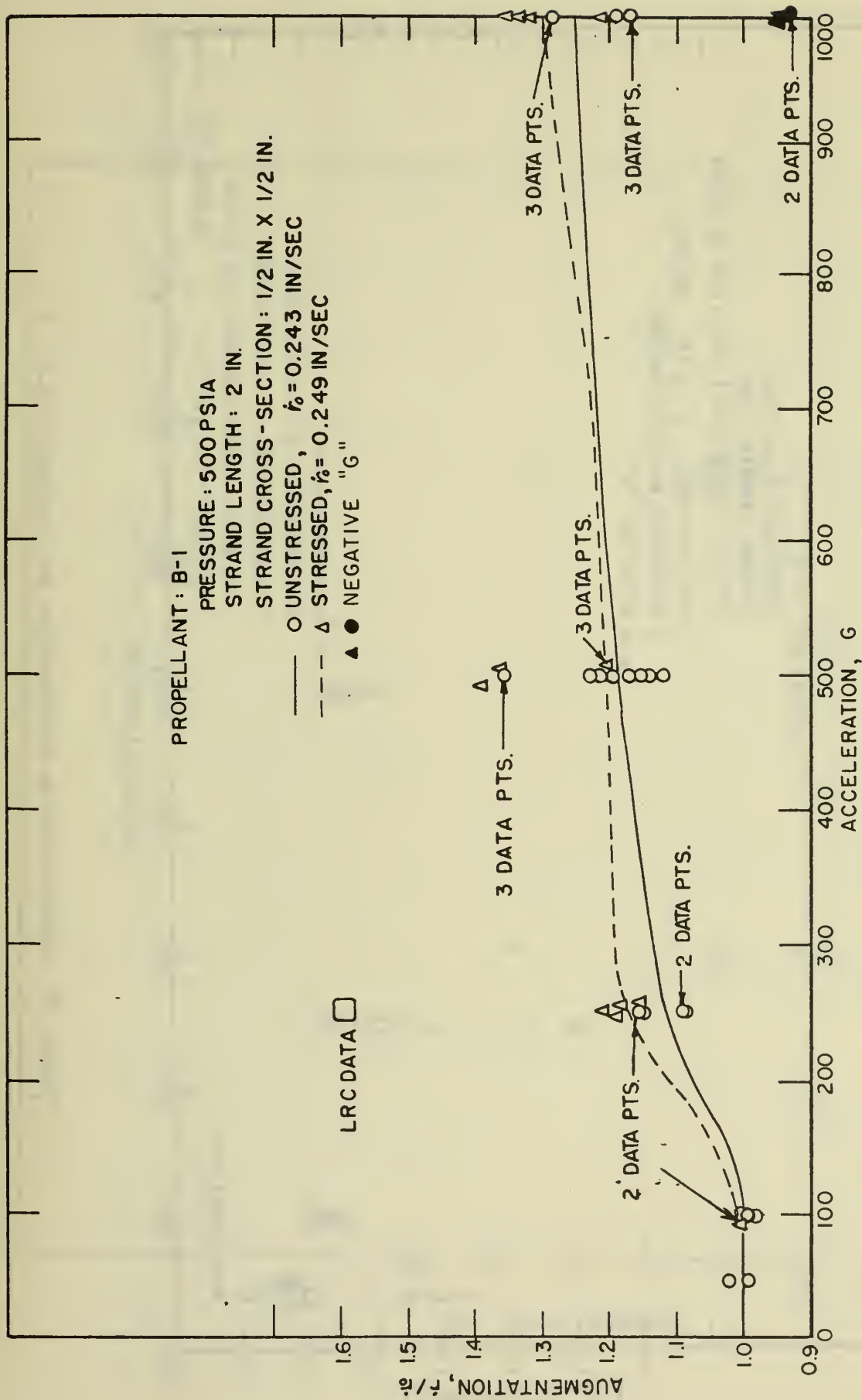


Figure 38 Augmentation vs Acceleration for Propellant B-1

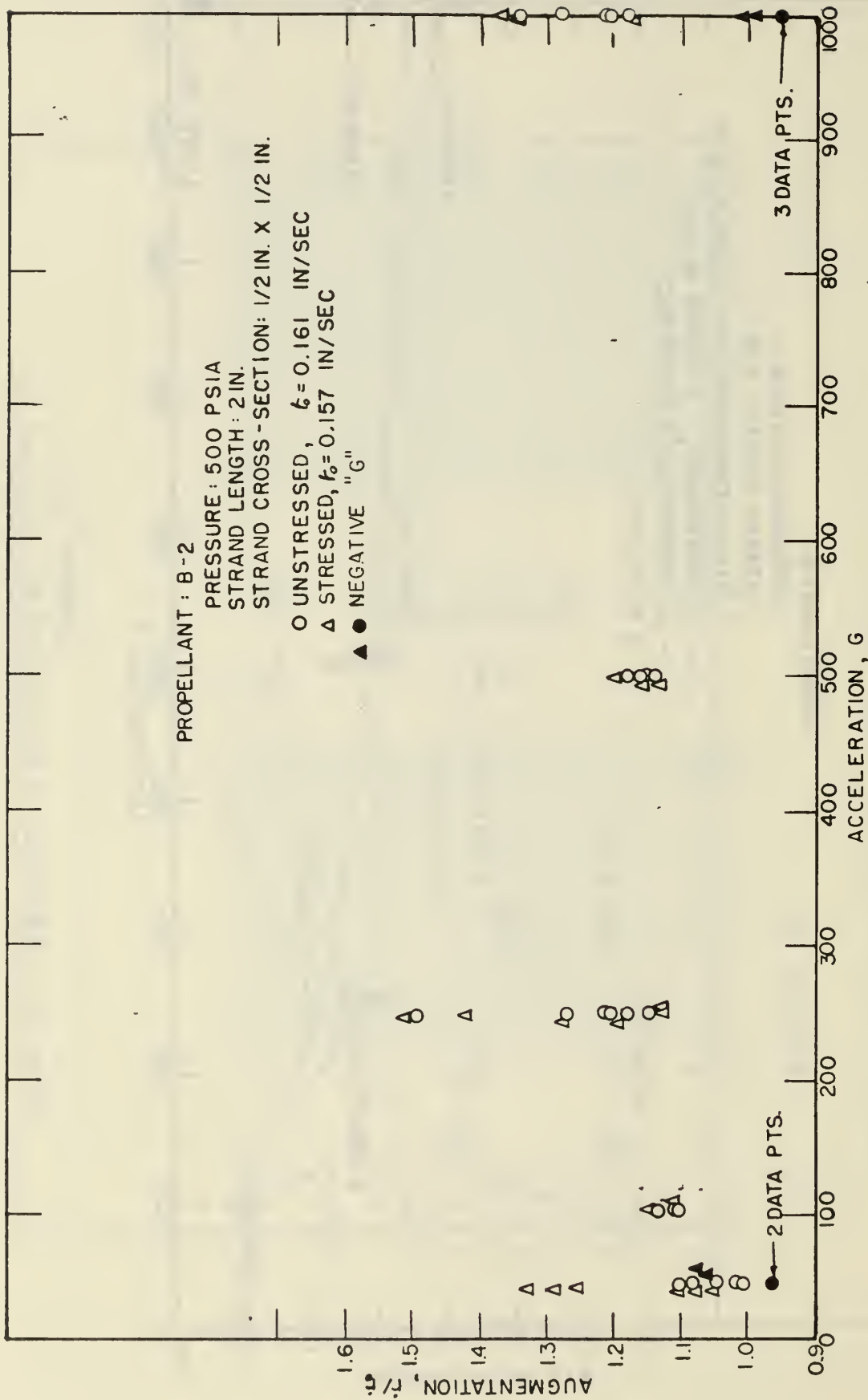


Figure 39 Augmentation vs Acceleration for Propellant B-2

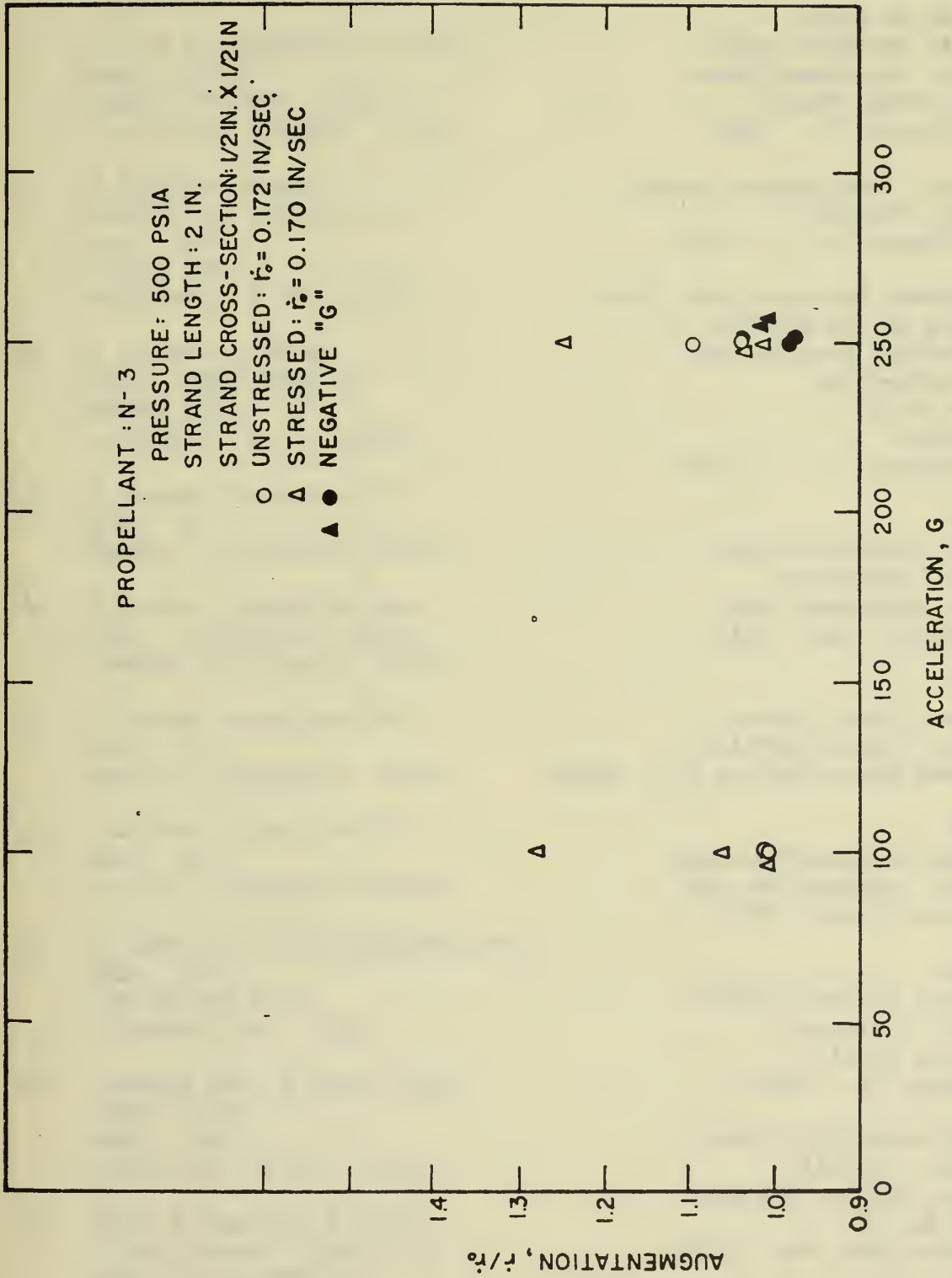


Figure 40 Augmentation vs Acceleration for Propellant N-3

DISTRIBUTION LIST

	No. Copies
1. Bureau of Mines Safety Research Center Attn: Documents Library 4800 Forbes Avenue Pittsburgh, Pa. 15213	1
2. Central Intelligence Agency Attn: CRS/ADD Washington, D. C. 20505	1
3. Assistant Director (Eng. Tech.) Office of the Director of Defense Research and Engineering Room 3D1085 Pentagon Washington, D. C. 20301	1
4. NASA Lewis Research Center Attn: Librarian 21000 Brookpark Road Cleveland, Ohio 44135	1
5. NASA Kennedy Space Center Attn: Library-ATS-132C Kennedy Space Center, Fla. 32899	1
6. NASA Manned Spacecraft Center Attn: Library/Code BM6 Houston, Texas 77058	1
7. NASA Langley Research Center Attn: Librarian Langley Station Hampton, Va. 23565	3
8. NASA Scientific & Tech. Info. Facility Attn: SAF/DL, ACQ Div. P.O. Box 33 College Park, Md. 20740	2

9. NASA 1
Attn: Code RPS
Washington, D. C. 20546
10. Defense Documentation Center 12
Attn: DDC-TCA
Cameron Station, Bldg. 5
Alexandria, Virginia 22314
11. AF Systems Command 1
Director of Laboratories
Attn: DLV
Andrews AFB
Washington, D. C. 20331
12. AF Systems Command 1
Attn: DPSL, Library
Andrews AFB
Washington, D. C. 20331
13. AF Rocket Propulsion Lab. 1
Attn: RT
Edwards, California 93523
14. AF Rocket Propulsion Lab. 1
Attn: Technical Library
Edwards, California 93523
15. AF Rocket Propulsion Lab. 1
Attn: LK
Edwards, California 93523
16. AF Rocket Propulsion Lab. 1
Attn: MK
Edwards, California 93523
17. AF Office of Scientific Research 1
Attn: SREP
1400 Wilson Blvd.
Arlington, Va. 22209
18. Armament Dev. & Test Center 1
(AFSC) 16325 C4
Attn. XRC
Eglin AFB, Florida 32542
19. Naval Scientific & Tech. 1
Info. Center (09481 84)
Attn: Code STIC-231
4301 Suitland Road
Washington, D. C. 20390

20. Army Ballistic Res. Labs 2
Attn: AMXBR-I
Aberdeen Proving Ground, Md. 21005
21. Army Research Office 1
Attn: CRD-AA-IP
Box CM. Duke Station
Durham, North Carolina 27706
22. Frankford Arsenal 1
Attn: C2500-Library-B51-2
(for Propellant & Expl. Section)
Philadelphia, Pa. 19137
23. Picatinny Arsenal 3
Scientific & Tech. Info. Br.
Technical Services Directorate
(PA Library)
Attn: SMUPA-TR-5, Bldg. 59
Dover, New Jersey 07801
24. Army Missile Command 4
Redstone Scientific Info. Center
Attn: Chief, Document Section
Redstone Arsenal, Alabama 35809
25. White Sands Missile Range 1
Attn: Technical Library
White Sands MR, New Mexico 88002
26. Naval Air Systems Command 1
Attn: AIR-6042, Tech. Library
Washington, D. C. 20360
27. Naval Air Systems Command 1
Attn: AIR-53664
Washington, D. C. 20360
28. Naval Ordnance Systems Command 1
Attn: ORD-55211B
Washington, D. C. 20360
29. Naval Ordnance Systems Command 1
Attn: ORD-0331
Washington, D. C. 20360
30. Naval Ordnance Laboratory 2
Attn: Library
White Oak
Silver Spring, Maryland 20910

- | | | |
|-----|---|---|
| 31. | Naval Air Systems Command
Attn: AIR-330
Washington, D. C. 20360 | 2 |
| 32. | Naval Weapons Center
Attn: Code 753-Technical Library
China Lake, California 93555 | 3 |
| 33. | Naval Postgraduate School
Attn: Library, Tech. Repts.
Section 2124
Monterey, California 93940 | 1 |
| 34. | Naval Ordnance Station
Attn: Technical Library
Indian Head, Maryland 20640 | 2 |
| 35. | Naval Research Branch Office
Attn: Librarian
1030 East Green Street
Pasadena, California 91101 | 1 |
| 36. | Naval Research
Attn: Code 473, Power Branch
Arlington, Va. 22217 | 1 |
| 37. | Naval Ordnance Systems Command
Attn: ORD-9132
Tech. Library
Washington, D. C. 20360 | 1 |
| 38. | Naval Research Lab.
Attn: Code 5117
Washington, D. C. 20390 | 1 |
| 39. | Navy Strategic Systems
Project Office
Attn: Technical Library
Munitions Bldg. Room 3245
Washington, D. C. 20360 | 1 |
| 40. | Naval Underwater Weapons
Res.-Eng. Sta.
Attn: Tech. Library (CS12)
Newport, R. I. 02840 | 1 |
| 41. | Naval Weapons Laboratory
Attn: Technical Library
Dahlgren, Virginia 22488 | 1 |

42. Aerojet-General Corp. 1
 Aerojet Liquid Rocket Co.
 Attn: Tech. Info. Ctr.
 P.O. Box 13222
 Sacramento, California 95813
43. Philco-Ford Corp. 1
 Aeronutronic Division
 Attn: Tech. Info. Svcs. Acquisitions
 Ford Road
 Newport Beach, California 92663
44. Aerospace Corp. 2
 Attn: Tech. Info. Ctr.-Doc. Group
 P.O. Box 95085
 Los Angeles, California 90045
45. Atlantic Research Corp. 2
 Attn: Library
 Shirley Highway at Edsall Road
 Alexandria, Va. 22314
46. Textron, Inc. 1
 Bell Aerosystems Co., Div.
 P.O. Box 1
 Buffalo, New York 14240
47. Boeing Co. 1
 Attn: Aerospace Library-8K-38
 P. O. Box 3999
 Seattle, Washington 98124
48. Chemical Propulsion Info. Agency 2
 Applied Physics Lab-JHU
 8621 Georgia Avenue
 Silver Spring, Md. 20910
49. Lockheed Missiles & Space Co. 1
 Attn: Tech. Info. Ctr., 50-14
 3251 Hanover Street
 Palo Alto, California 94304
50. Hercules, Inc. 1
 Allegany Ballistics Lab.
 Attn: Technical Library
 P.O. Box 210
 Cumberland, Md. 21502
51. Hercules, Inc. 1
 Research Center
 Attn: Tech. Info. Center
 Wilmington, Delaware 19899

52. Institute for Defense Analyses 1
 Attn: Classified Library
 400 Army-Navy Drive
 Arlington, Virginia 22202
53. California Inst. of Technology 1
 Jet Propulsion Laboratory
 Attn: Library, TDS
 4800 Oak Grove Drive
 Pasadena, California 91103
54. Lockheed Propulsion Co. 2
 Attn: Library
 P.O. Box 111
 Redlands, California 92373
55. CCI Aerospace Corp. 0008 F4 1
 Marquardt Co. Div.
 Attn: Library
 P.O. Box 2013, So. Annex
 Van Nuys, California 91409
56. Martin-Marietta Corp. 1
 Attn: MP-30, Engineering Library
 P.O. Box 5837
 Orlando, Florida 32805
57. North American Rockwell 1
 Space & Information Systems Div.
 Attn: Tech. Info. Ctr.-096-722
 12214 Lakewood Blvd.
 Downey, California 90241
58. Rocket Research Corp. 1
 Attn: Technical Library
 Willow Road at 116th Street
 Redmond, Washington 98052
59. North American Rockwell 1
 Rocketdyne Division
 Attn: Library Dept. 086-306
 6633 Canoga Avenue
 Canoga Park, California 91304
60. Rohm & Haas Co. 00660 F4 1
 Huntsville Defense Contract Office
 Attn: Security Office
 MIC Bldg No. 2
 1312 Meridian Street
 Huntsville, Alabama 35801

61. TRW Systems, Inc. 2
 Attn: Technical Info. Center
 One Space Park
 Redondo Beach, California 90278
62. Thiokol Chemical Corp. 1
 Huntsville Division
 Attn: Technical Library
 Huntsville, Alabama 35807
63. Thiokol Chemical Corp 1
 Elkton Division
 Attn: Tech. Info. Center
 Elkton, Md. 21921
64. Thiokol Chemical Corp. 2
 Wasatch Division
 Attn: Technical Library
 Brigham City, Utah 84302
65. United Aircraft Corp. 1
 Attn: Acquisitions Librarian
 400 Main Street
 East Hartford, Conn. 06108
66. United Aircraft Corp. 1
 Pratt & Whitney Aircraft Div.
 Attn: Head Librarian
 P.O. Box 2691
 West Palm Beach, Florida 33402
67. United Aircraft Corp. 1
 United Technology Center
 Attn: Technical Library
 P.O. Box 358
 Sunnyvale, California 94088
68. Princeton University 1
 Forrestal Campus Library
 Attn: Librarian
 P.O. Box 710
 Princeton, N. J. 08540
69. LTV Aerospace Corp. 1
 Missiles & Space Division
 Attn: Librarian-3-51000
 P.O. Box 6267
 Dallas, Texas 75222
70. Aerojet-General Corp. 1
 Aerojet Solid Propulsion Co.
 Attn: Library
 P.O. Box 13400
 Sacramento, California 95813

71. McDonnell Douglas Corp. 1
 Missile and Space Div.
 Attn: A3-328 Library Services
 5301 Bolza Ave.
 Huntington Beach, California 92646
72. Army Ammo. Procurement 1
 & Supply Agency
 Attn: RDL, Quality Assurance
 Tech. Library
 Joliet, Illinois 60431
73. Army Ammunition Plant 1
 Attn: SMURO-IN
 Radford, Virginia 24141
74. McDonnell Douglas Corp. 1
 Attn: Library
 P.O. Box 516
 St. Louis, Missouri 63166
75. Hercules, Inc. 1
 Bacchus Works
 Attn: Library 100-H-2
 P.O. Box 98
 Magna, Utah 84044
76. Olin Mathieson Chemical Corp. 1
 Attn: Asst. Librarian
 Mail Control Room
 275 Winchester Avenue
 New Haven, Conn. 06504
77. North American Rockwell 1
 Rocketdyne Division
 Attn: Library
 McGregor, Texas 76657
78. Shell Oil Co. 1
 Shell Development Co. Div.
 Attn: Technical Files
 1400 53rd Street
 Emeryville, California 94608
79. Martin-Marietta Corp. 1
 Attn: Research Library, 6617
 P.O. Box 179
 Denver, Colorado 80201

- | | | |
|-----|---|----|
| 80. | Dean of Research Administration
Code 023
Naval Postgraduate School
Monterey, California 93940 | 2 |
| 81. | Chairman
Department of Aeronautics
Naval Postgraduate School
Monterey, California 93940 | 1 |
| 82. | D. W. Netzer
Department of Aeronautics
Naval Postgraduate School
Monterey, California 93940 | 10 |
| 83. | J. R. Kennedy
Department of Aeronautics
Naval Postgraduate School
Monterey, California 93940 | 1 |
| 84. | G. M. Biery, II
Department of Aeronautics
Naval Postgraduate School
Monterey, California 93940 | 1 |
| 85. | W. E. Brown
Department of Aeronautics
Naval Postgraduate School
Monterey, California 93940 | 1 |

DOCUMENT CONTROL DATA - R & D

(Security classification of title, body of abstract and indexing annotation must be entered when the overall report is classified)

1. ORIGINATING ACTIVITY (Corporate author) Naval Postgraduate School Monterey, California 93940		2a. REPORT SECURITY CLASSIFICATION UNCLASSIFIED	
		2b. GROUP	
3. REPORT TITLE Nonmetallized Composite Propellant Combustion			
4. DESCRIPTIVE NOTES (Type of report and, inclusive dates) Technical Report, 1971			
5. AUTHOR(S) (First name, middle initial, last name) D. W. Netzer, J. R. Kennedy, G. M. Biery II, W. E. Brown			
6. REPORT DATE 1 March 1972		7a. TOTAL NO. OF PAGES 121	7b. NO. OF REFS 36
8a. CONTRACT OR GRANT NO. ORD-331-007/551-1/UF 19-332-303		9a. ORIGINATOR'S REPORT NUMBER(S) NPS-57NI72031A	
b. PROJECT NO.		9b. OTHER REPORT NO(S) (Any other numbers that may be assigned this report)	
c.			
d.			
10. DISTRIBUTION STATEMENT Approved for public release; distribution unlimited.			
11. SUPPLEMENTARY NOTES		12. SPONSORING MILITARY ACTIVITY	
13. ABSTRACT An experimental investigation of nonmetallized composite propellant combustion in standard and high acceleration environments was made. Pressed ammonium perchlorate (AP) pellets of varying purity, AP/binder sandwich burners, and propellant strands were employed. AP/binder sandwich burners were studied in an optically equipped centrifuge and color schlieren were taken in a conventional combustion bomb. Ascast and dewetted propellants were used to study the effect of preferential interfacial reactions on burning rate acceleration sensitivity. Results are discussed for the effects of acceleration, pressure, AP purity, and propellant composition on the burning rate.			

14 KEY WORDS	LINK A		LINK B		LINK C	
	ROLE	WT	ROLE	WT	ROLE	WT
Solid Propellant						
Composite, Sandwich, AP						
Burning Rate						
Acceleration						
Pressure						

U144635

DUDLEY KNOX LIBRARY - RESEARCH REPORTS



5 6853 01069464 9

